Residence time estimates for asymmetric simple exclusion dynamics on strips

Emilio N.M. Cirillo
Dipartimento di Scienze di Base e Applicate per l'Ingegneria, Sapienza Università di Roma, via A. Scarpa 16, I–00161, Roma, Italy.
E_mail: emilio.cirillo@uniroma1.it

Oleh Krehel
Institute of Complex Molecular Systems and Faculty of Chemical Engineering, Eindhoven University of Technology, P.O. Box 513, 5600 MB Eindhoven, The Netherlands
E_mail: o.krehel@tue.nl

Adrian Muntean
Department of Mathematics and Computer Science, (CASA) Centre for Analysis, Scientific computing and Applications, Institute for Complex Molecular Systems Eindhoven University of Technology, P.O. Box 513, 5600 MB Eindhoven, The Netherlands
E_mail: a.muntean@tue.nl

Rutger van Santen
Institute of Complex Molecular Systems and Faculty of Chemical Engineering, Eindhoven University of Technology, P.O. Box 513, 5600 MB Eindhoven, The Netherlands
E_mail: R.A.v.Santen@tue.nl

Aditya Sengar
Indian Institute of Technology Delhi, India
E_mail: adityasengariitd@gmail.com

Abstract. The target of our study is to approximate numerically and, in some particular physically relevant cases, also analytically, the residence time of particles undergoing an asymmetric simple exclusion dynamics on a two–dimensional vertical strip. The sources of asymmetry are twofold: (i) the choice of boundary conditions (different reservoir levels) and (ii) the strong anisotropy from a drift nonlinear in density with prescribed directionality. We focus on the effect of the choice of anisotropy on residence time. We analyze our results by means of two theoretical models, a Mean Field and a one–dimensional Birth and Death one. For positive drift we find a striking agreement between Monte Carlo and theoretical results. In the zero drift case we still find agreement as long as particles can freely escape the strip through the bottom boundary. Otherwise, the two models give different predictions and their ability to reproduce numerical results depend on the horizontal displacement probability.

The topic is relevant for situations occurring in pedestrian flows or biological transport in crowded environments, where lateral displacements of the particles occur predominantly affecting therefore in an essentially way the efficiency of the overall transport mechanism.

Pacs: 05.40.Fb; 02.70.Uu; 64.60.ah

MSC Classification: 82B41; 82B21; 82B43; 82B80; 60K30; 60K35; 90B20

Keywords: residence time, simple exclusion random walks, deposition model, complexity, self–organization

1. Introduction

The efficiency of transport of active matter in microscopic systems is an issue of paramount importance in a number of fields of science including biology, chemistry, and logistics. Looking particularly at drug–delivery design scenarios [23], ion moving in molecular cytosol [2–4], percolation of aggressive acids through reactive porous media [18], the traffic of pedestrians in regions with drastically reduced visibility (e.g., in the dark or in the smoke) [11,12,25] (see also the problem of traffic of cars on single–lane highways [28]), we see that the efficiency of a medical treatment, the properties of ionic currents thorough cellular membranes, the durability of a highly permeable material, or the success of the evacuation of a crowd of humans, strongly depends on the time spent by the individual particle (colloid, ion, acid molecule, or human being) in the constraining geometry (body, molecule, fabric, or corridor).

In this framework, we focus our attention on the study of the simplest 2D scenario that mimics alike dynamics. The *Gedankenexperiment* we make is the following: we imagine a vertical strip whose top and bottom entrances are in touch with infinite particle reservoirs at constant densities. Assume particles are driven downwards by the boundary densities difference and/or an external constant and uniform field (electrical, gravitational, generally–accepted crowd opinion, ...). Let the *residence time* be the typical time a particle entering the strip at stationarity from the top boundary needs to exit through the bottom one. In this framework, under the assumption that particles in the strip interact only via hard–core exclusion, we study the *ballistic–like* versus the *diffusion–like* dependence of the residence time on the external driving force (main source of anisotropy in the system), on the length of the strip, on the horizontal diffusion, and, finally, on the choice of the boundary condition at the bottom.

We recover the structure of the fluxes as well as the residence times proven mathematically by Derrida and co–authors in [14] for the asymmetric simple exclusion model on the line; see also [21] for a more recent approach. In chemistry single file diffusion has been demonstrated

for zeolite catalysts [22] to dramatically reduce the rate of a reaction. This happens in particular when zeolitic microporous systems are used with linear micropores with dimensions that are similar as the size of the molecules that are converted. Since they cannot pass single file inhibition occurs (see, for instance, [20]).

Additionally, we discover new effects that are purely due to the choice of the 2D geometry and which are therefore absent in a 1D lattice. The most prominent, within the precision of our numerical simulations, is the non–monotonic behavior in changes in the horizontal displacement probability in the bouncing back regime reported in Section 6.3. Under certain conditions, particles start accumulating near the bottom exit of the strip. This crowding leads to a bouncing-back effect in which particles trying to escape are reflected in the bulk. We observe that, in such a case, increasing the frequency of horizontal movements help particles to overcome obstacles and to find their way to the exit.

To investigate this model, we employ several working techniques including Taylor series truncations for the derivation of the mean–field equations, ODE analysis of the stationary case, estimates involving the structure of the stationary measure for birth and death processes on a line, as well as Monte Carlo simulations to exploit the resources offered by the various parameter regimes. In 1D, this model has been widely studied both by the mathematical and physical communities, see e.g. [7, 8, 14, 16, 21, 26]. In 2D, the situation is very much unexplored especially in the asymmetric case. We deal with this precise problem and we give a rather complete description of the phenomenon. Our results, which are based on a thorough study of two simplified models and extensive Monte Carlo simulations, open new mathematical problems concerning the typical time a particle need to cross a region in hard–core repulsion regime.

More precisely, in the paper we develop two analytic approaches to predict the mean residence time: a macroscopic Mean Field theory and a semi–microscopic approach in which the particle motion is imagined as that of a single particle against a prescribed background density profile borrowed from the macroscopic Mean Field theory. These two different predictions are very similar to each other but for the regime described above in which the non–monotonic effect is found. In this regime the horizontal displacement probability tunes the system behavior from the macroscopic prediction to the semi–microscopic one, with the two limits recovered, respectively, in the zero and one horizontal probability displacement cases.

The importance of the exclusion rule on the time dependence of the typical distance covered by a particle is not new in the scientific literature. Due to the exclusion rule, the asymmetric process on a square lattice that we discuss here can be considered to occur on a percolating lattice. The symmetric exclusion case has been widely explored for diffusion,

as for instance the "ant in the labirinth" by de Gennes [1]. The distance travelled by the ant is proportional to the square root of the time (random walk diffusion) as long as the site occupancy is low, but, when the critical 0.5928 site occupation is approached, this changes to a time dependence close to cubic root of time. Beyond this critical site occupancy the order in time rapidly drops. The excluded volume problem in several dimensions has not yet found however a satisfactory solution [15].

A related but similar phenomenon occurs in the symmetric 1D case. When site occupation increases the distance time relation becomes the fourth root of time [19]. The asymmetric problem in 2D, that we are interested in, can be more easily addressed as asymmetric exclusion with driven diffusion, see [24] for a paper and [9] for a complete review. In the 1D total asymmwtric case (particles can move only from the top to the bottom), using a kinematic wave theory related approach and the method of maximum transported current [9], it is identified a three parameter space region as a function of the rates at which particles would enter (from the top) or exit (from the bottom) the strip. These regions closely relate to the particle density where percolation sets in (on a square lattice with stochastic bond formation the percolation threshold is 0.5). In this paper we will be mainly concerned with the case where the relative probability for a particle to enter the strip (from the top) is one. In this case the two situations than can be distinguished are the high density phase (exit probability smaller than 1/2) and the maximum current phase (exit probability larger than 1/2). Interestingly the difference relates to an occupation density that is larger or less than the critical point of percolation.

In the lower density phase the average density is 1/2 and current is maximum, at the density higher than the percolation threshold it decreases with the exit rate. [9]. We derive an equation for the Mean Field concentration profile which, in our setup, depends only on the vertical spatial coordinate. The profile depends on the reservoir boundary conditions and on the vertical drift, namely, the ratio between down and up jump probabilities divided by their sum, that, we recall, we do not considered necessarily equal to one (as in the total asymmetric case discussed above). In the large drift case, we recover density profiles consistent with the phase diagram described above which has been proven to be correct in the total asymmetric case [14].

In this scenario, as already mentioned above, we setup two different analytic computations of the residence time: a semi–microscopic approach based on the analogy with a 1D birth and death model with not homogeneous background and a purely macroscopic Mean Field approximation. In the last approach the residence time is finally computed in terms of the stationary current. It is important to stress that, for zero drift, these two different approach seem to explain the behavior of the model in two different regimes, namely, low and high

horizontal displacement probability. From our point of view this result is of absolutely high interest, indeed, the main issue we arise in this paper is that of understanding the influence of lateral displacements on the typical time needed by a particle to cross a strip. Future investigation will be needed to understand deviations from the average particle behavior. In this perspective the residence time seems to be a very useful observable and its distribution will be the key object of our future study.

The paper is structured in the following fashion: we describe the dynamics of our stochastic lattice model in Section 2. Section 3 is concerned primarily with the derivation of the mean field equations governing the macroscopic evolution of the density. In the same section we study the stationary mean field behavior, the thermalization time of the system (i.e. the time that the system takes to reach the steady state) as well as the numerical testing of the accuracy of the mean field prediction of the stationary density profile. In Section 4 we make the direct analogy between our scenario and a biased birth and death model for which we can calculate explicitly the unique invariant measure and the use this object to obtain analytical lower and upper bounds on the residence time for three distinct physically relevant scenarios, viz. (i) a homogeneous case, (ii) a linear case, (iii) a totally asymmetric case. The core of the paper is Section 5 and Section 6. Herein we use inspiration from the handling of the biased birth and death model to get approximate analytical bounds on the residence time for our problem for selected parameter regimes. We also setup a purely Mean Field macroscopic computation yielding a prediction of the residence time which is fully discussed in the last two sections.Finally, we explore numerically the residence time for all parameter regimes and compare the results with the derived analytical bounds.

2. The model

Let L_1, L_2 be two positive integers. Let $\Lambda \subset \mathbb{Z}^2$ denote the *strip* $\{1, \dots, L_1\} \times \{1, \dots, L_2\}$. We say that the coordinate directions 1 and 2 of the strip are respectively the *horizontal* and the *vertical* direction. We shall accordingly use the words *top*, *bottom*, *left*, and *right*. On Λ we define a discrete time stochastic process controlled by the parameters

$$\varrho_{\mathrm{u}}, \varrho_{\mathrm{d}} \in [0,1] \quad \text{and} \quad h, u, d \in [0,1] \quad \text{such that } h + u + d = 1$$

whose meaning will be explained below.

The *configuration* of the system at time $t \in \mathbb{Z}_+$ is given by the positive integer $n(t)$ denoting the number of particles in the system at time t and by the two collections of integers $x_1(1,t), \dots, x_1(n(t),t) \in \{1, \dots, L_1\}$ and $x_2(1,t), \dots, x_2(n(t),t) \in \{1, \dots, L_2\}$ denoting, respectively, the horizontal and the vertical coordinates of the $n(t)$ particles in the strip Λ at time t. The i–th particle, with $i = 1, \dots, n(t)$, is then associated with the site

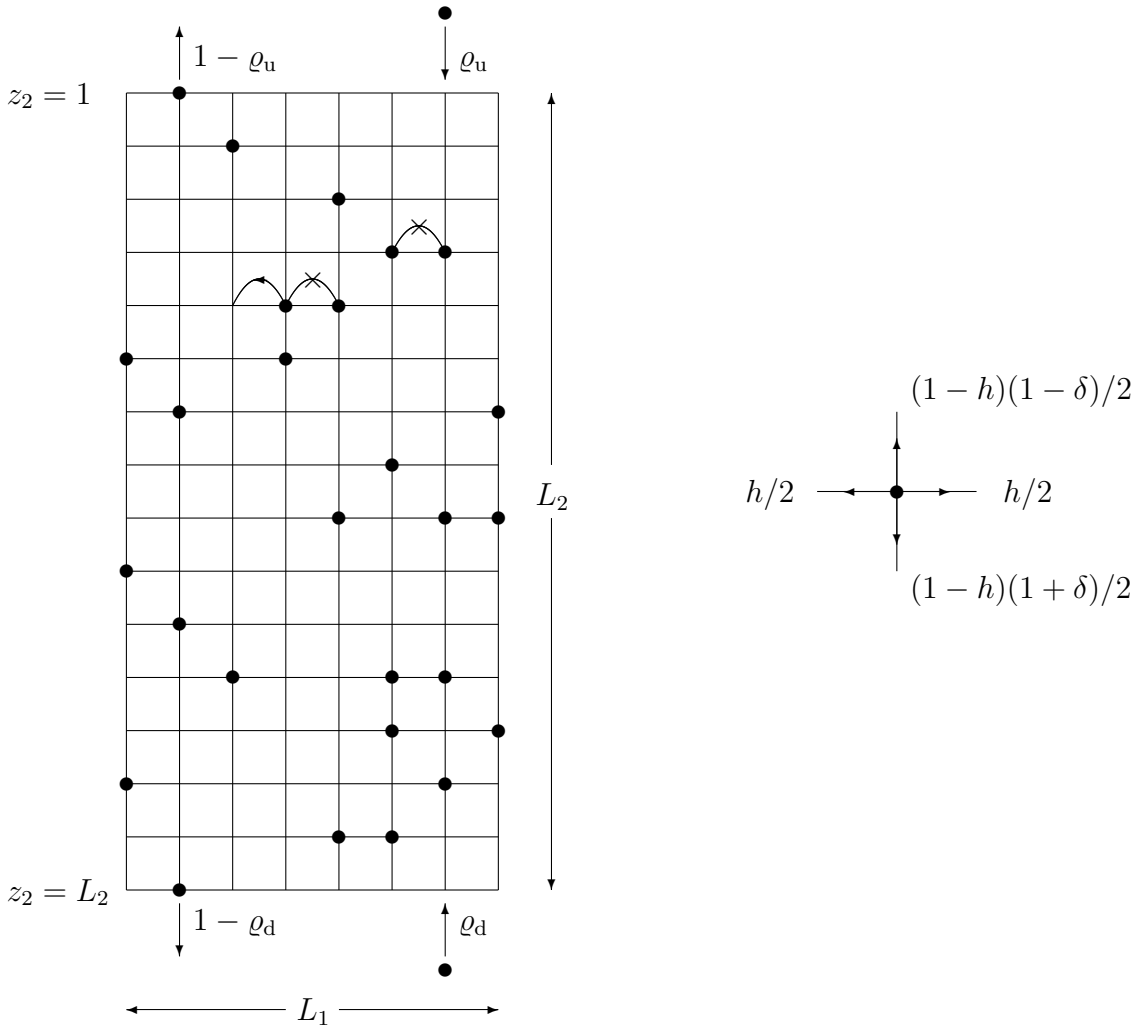

Figure 1.1: Schematic representation of the model: the lattice on the left and the jumping probabilites on the right.

$(x_1(i,t), x_2(i,t)) \in \Lambda$ which is called *position* of the particle at time t. A site associated with a particle a time t will be said to be *occupied* at time t, otherwise we shall say that it is *free* or *empty* at time t. We let $n(0) = 0$.

At each time $t \geq 1$ we first set $n(t) = n(t-1)$ and then repeat the following algorithm $n(t-1)$ times. Essentially, at each step of the dynamics, a number of particles equal to the number of particles in the system at the end of the preceding time $n(t-1)$ is tentatively moved. One of the three actions *insert a particle through the top boundary*, *insert a particle through the bottom boundary*, and *move a particle in the bulk* is performed with the corresponding probabilities $\varrho_{\rm u}L_1/(\varrho_{\rm u}L_1+\varrho_{\rm d}L_1+n(t))$, $\varrho_{\rm d}L_1/(\varrho_{\rm u}L_1+\varrho_{\rm d}L_1+n(t))$, and $n(t)/(\varrho_{\rm u}L_1+\varrho_{\rm d}L_1+n(t))$.

Insert a particle through the top boundary. Chose at random with uniform probability the integer $i \in \{1, \dots, L_1\}$ and, if the site $(1, i)$ is empty, with probability d set $n(t) = n(t) + 1$ and add a particle to site $(1, i)$.

Insert a particle through the bottom boundary. Chose at random with uniform probability the integer $i \in \{1, \dots, L_1\}$ and, if the site (L_2, i) is empty, with probability u set $n(t) = n(t) + 1$ and add a particle to site (L_2, i).

Move a particle in the bulk. Chose at random with uniform probability one of the $n(t)$ particles in the bulk. The chosen particle is moved according to the following rule: one of the four neighboring sites of the one occupied by the particle is chosen at random with probability $h/2$ (left), u (up), $h/2$ (right), and d (down). If the chosen site is in the strip (not on the boundary) and it is free, the particle is moved there leaving empty the site occupied at time t. If the chosen site is on the boundary of the strip the dynamics is defined as follows: the left boundary $\{(0, z_2),\ z_2 = 1, \dots, L_2\}$ and the right boundary $\{(L_1 + 1, z_2),\ z_2 = 1, \dots, L_2\}$ are *reflecting* (homogeneous Neumann boundary conditions) in the sense that a particle trying to jump there is not moved. The bottom and the top boundary conditions are stochastic in the sense that when a particle tries to jump to a site $(z_1, 0)$, with $z_1 = 1, \dots, L_1$, such a site has to be considered occupied with probability ϱ_{u} and free with probability $1 - \varrho_{\mathrm{u}}$, whereas when a particle tries to jump to a site $(z_1, L_2 + 1)$, with $z_1 = 1, \dots, L_1$, such a site has to be considered occupied with probability ϱ_{d} and free with probability $1 - \varrho_{\mathrm{d}}$. If the arrival site is considered free the particle trying to jump there is removed by the strip Λ (it is said to *exit* the system) and the number of particles is reduced by one, namely, $n(t) = n(t) - 1$. If the arrival site is occupied the particle is not moved.

We gave the definition of the model in an algorithmic way, but note that the model is a Markov chain $\omega_0, \omega_1, \dots, \omega_t, \dots$ on the *state* or *configuration space* $\Omega := \{0, 1\}^\Lambda$ with transition probability that can be deduced by the algorithmic definition.

3. Mean Field estimates

Let the *occupation number* of the site $(z_1, z_2) \in \Lambda$ at time t be equal to 1 if such a site is occupied by a particle at time t and to 0 otherwise. Let, also, $m_t(z_1, z_2)$ be the expectation of the occupation number at site $(z_1, z_2) \in \Lambda$ at time $t \geq 0$. This quantity is well defined in a stochastic context. But if one wants a more intuitive idea of what such a quantity is, one can think of running the dynamics many times independently and then computing equal time averages with respect to these different realizations of the process. The mean over those independent realizations of the occupation number at site (z_1, z_2) at time t will be $m_t(z_1, z_2)$.

Now, we set up a Mean Field computation for such a mean occupation time m_t. We shall follow [27], but it is worth noting that, in 1D and on the infinite volume $\mathbb{Z}$, the equation we

shall obtain is proven rigorously to be the macroscopic limit of the discrete space random process [13].

We need to reproduce and slightly generalize the approach in [27] since there a particular choice for the horizontal probability has been considered, whereas we need a more general result. Let the *drift* be

$$\delta = \frac{d-u}{d+u} \quad . \tag{3.1}$$

This is indeed the physically meaningful definition of drift, since it is the ratio between the difference of the probabilities to move down and up and the total probability to perform a vertical displacement. Note that, since $d+u = 1-h$, a simple computation yields

$$d = \frac{1-h}{2}(1+\delta) \quad \text{and} \quad u = \frac{1-h}{2}(1-\delta) \quad . \tag{3.2}$$

First of all, note that in our dynamics the probability that at time t a specific particle is updated is of order one, since at each time we update at random $n(t-1)$ particles, where, we recall, $n(t)$ is the number of particles in the system at time t. Thus, the Mean Field approximation consists in letting

$$\varepsilon = \frac{1}{L_2+1} \quad \text{and} \quad \tau = \varepsilon^2 \ , \tag{3.3}$$

considering the macroscopic variables

$$z_1' = \varepsilon z_1, \quad z_2' = \varepsilon z_2, \qquad \text{and} \quad t' = \tau t = \varepsilon^2 t \ , \tag{3.4}$$

and writing, for an arbitrary point in the bulk, the following balance equation:

$$\begin{aligned}
&m_{t'+\tau}(z_1', z_2') - m_{t'}(z_1', z_2') \\
&\quad = (h/2) m_{t'}(z_1'-\varepsilon, z_2')[1 - m_{t'}(z_1', z_2')] + d m_{t'}(z_1', z_2'-\varepsilon)[1 - m_{t'}(z_1', z_2')] \\
&\qquad + (h/2) m_{t'}(z_1'+\varepsilon, z_2')[1 - m_{t'}(z_1', z_2')] + u m_{t'}(z_1', z_2'+\varepsilon)[1 - m_{t'}(z_1', z_2')] \\
&\qquad - (h/2) m_{t'}(z_1', z_2')[1 - m_{t'}(z_1'+\varepsilon, z_2')] - d m_{t'}(z_1', z_2')[1 - m_{t'}(z_1', z_2'+\varepsilon)] \\
&\qquad - (h/2) m_{t'}(z_1', z_2')[1 - m_{t'}(z_1'-\varepsilon, z_2')] - u m_{t'}(z_1', z_2')[1 - m_{t'}(z_1', z_2'-\varepsilon)] \\
&\quad = (h/2)[m_{t'}(z_1'+\varepsilon, z_2') - 2m_{t'}(z_1', z_2') + m_{t'}(z_1'-\varepsilon, z_2')] \\
&\qquad + ((1-h)/2)[m_{t'}(z_1', z_2'+\varepsilon) - 2m_{t'}(z_1', z_2') + m_{t'}(z_1', z_2'-\varepsilon)] \\
&\qquad - \delta((1-h)/2)\{[1 - m_{t'}(z_1', z_2')][m_{t'}(z_1', z_2'+\varepsilon) - m_{t'}(z_1', z_2'-\varepsilon)] \\
&\qquad\qquad + m_{t'}(z_1', z_2')[(1 - m_{t'}(z_1', z_2'+\varepsilon)) - (1 - m_{t'}(z_1', z_2'-\varepsilon))]\} \quad .
\end{aligned}$$

Now, we multiply and divide suitably the space and time units ε and τ to obtain

$$\begin{aligned}
&[m_{t'+\tau}(z_1', z_2') - m_{t'}(z_1', z_2')]/\tau \\
&\quad = (h/2)\,[m_{t'}(z_1'+\varepsilon, z_2') - 2m_{t'}(z_1', z_2') + m_{t'}(z_1'-\varepsilon, z_2')]/\varepsilon^2 \\
&\qquad + [(1-h)/2]\,[m_{t'}(z_1', z_2'+\varepsilon) - 2m_{t'}(z_1', z_2') + m_{t'}(z_1', z_2'-\varepsilon)]/\varepsilon^2 \\
&\qquad - [\delta(1-h)/\varepsilon]\,\{[1 - m_{t'}(z_1', z_2')][m_{t'}(z_1', z_2'+\varepsilon) - m_{t'}(z_1', z_2'-\varepsilon)] \\
&\qquad\qquad + m_{t'}(z_1', z_2')[(1 - m_{t'}(z_1', z_2'+\varepsilon)) - (1 - m_{t'}(z_1', z_2'-\varepsilon))]\}/(2\varepsilon) \quad .
\end{aligned}$$

Finally, if we assume that in the limit $\varepsilon \to 0$, namely, $L_2 \to \infty$, the drift scales to zero as

$$\delta = \varepsilon \bar{\delta} \ ,$$

we find the Mean Field limiting equation

$$\frac{\partial m_{t'}}{\partial t'} = \frac{1}{2} h \frac{\partial^2 m_{t'}}{\partial {z_1'}^2} + \frac{1}{2}(1-h)\frac{\partial^2 m_{t'}}{\partial {z_2'}^2} - \bar{\delta}(1-h)\frac{\partial}{\partial z_2'}[m_{t'}(1-m_{t'})] \ . \tag{3.5}$$

It is worth noting that the above equation is a diffusion–like equation with a nonlinear anisotropic flux. From the physical point of view the most interesting remark is that the diffusion part of the equation is linear. The effect of the drift is captured in nonlinear transport term. This term vanishes when $\bar{\delta} = 0$, so that linearity is approximatively restored at very small $\bar{\delta}$. It is worth noting that, by the choice of scaling, there is no inbuilt bias towards diffusion- or drift-alone.

To compare the solution of the Mean Field equation to the numerical simulations, we abuse the notation (recall that t, z_1, and z_2 denoted above integer numbers) and write $t = t'/\tau$, $z_1 = z_1'/\varepsilon$, and $z_2 = z_2'/\varepsilon$. The above limiting equation then reads

$$\frac{\partial m_t}{\partial t} = \frac{1}{2} h \frac{\partial^2 m_t}{\partial z_1^2} + \frac{1}{2}(1-h)\frac{\partial^2 m_t}{\partial z_2^2} - \delta(1-h)\frac{\partial}{\partial z_2}[m_t(1-m_t)] \ . \tag{3.6}$$

Since in the top and bottom boundary densities are constant in space (along the border), the stationary solutions to (3.6) do not depend on the space variable z_1. We call $\varrho(z_2)$ a *density profile* of the stationary Mean Field equation

$$\frac{d^2}{dz_2^2}\varrho - b\frac{\mathrm{d}}{\mathrm{d}z_2}\varrho(1-\varrho) = 0 \quad \text{with} \quad b = \frac{2\delta(1-h)}{1-h} = 2\delta \tag{3.7}$$

with the Dirichlet boundary conditions

$$\varrho(0) = \varrho_{\mathrm{u}} \quad \text{and} \quad \varrho(L_2+1) = \varrho_{\mathrm{d}} \ . \tag{3.8}$$

3.1. Stationary Mean Field behavior

Finding the stationary profile $\varrho(z_2)$ means solving the ordinary differential equation (3.7) with the Dirichlet boundary conditions (3.8). In the case $\delta = 0$ the solution is trivially linear. We now discuss the case $\delta > 0$. We integrate equation (3.7) once with respect to the space variable from 0 to z_2 to get

$$\varrho' = b\varrho(1-\varrho) + c \quad \text{where} \quad c = \varrho'(0) - b\varrho_{\mathrm{u}}(1-\varrho_{\mathrm{u}}) \ . \tag{3.9}$$

The structure of the solutions of this equation, namely the phase space trajectories, can be studied via a simple qualitative analysis (see, for instance, [5, Chapter 1]). Let

$f(\varrho) = b\varrho(1-\varrho) + c$ be the right hand side of (3.9). Five different situations have to be considered: $c > 0$, $c = 0$, $c < 0$ and $b/4+c > 0$, $b/4+c = 0$, and $b/4+c < 0$. In Figure 3.2 the phase diagram in the extended phase space is shown in the two cases $c < 0$ and $b/4 + c > 0$, $b/4 + c < 0$.

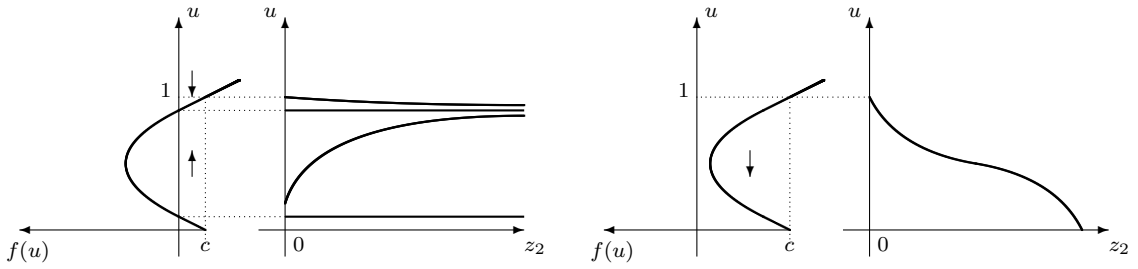

Figure 3.2: Phase diagram corresponding to (3.7). The case $c < 0$ and $b/4 + c > 0$ is depicted on the left. The case $b/4 + c < 0$ is depicted on the right.

Now, we find the solution of the stationary equation in the cases of interest. From the picture it is clear that:

- if $1 \geq \varrho_{\rm u} > 1/2 > \varrho_{\rm d} \geq 0$ the constant c has to be such that $b/4 + c < 0$;
- if $1 \geq \varrho_{\rm u} > \varrho_{\rm d} > 1/2$ the constant c has to be such that either $b/4 + c < 0$ or $0 > c > -b/4$.

It is important to remark that in the first case the constant c has to be necessarily larger that $-b/4$, while in the second case there are two different possibilities, so that we will have to decide which is the correct one.
Case $1 \geq \varrho_u > 1/2 > \varrho_d \geq 0$. Assume $b/4 + c < 0$, by performing a standard computation we find the solution

$$\arctan \frac{\varrho(z_2) - 1/2}{\sqrt{-c/b - 1/4}} = \arctan \frac{\varrho_{\rm u} - 1/2}{\sqrt{-c/b - 1/4}} - b\sqrt{-\frac{c}{b} - \frac{1}{4}}\, z_2 \tag{3.10}$$

with the constant c given by

$$\arctan \frac{\varrho_{\rm u} - 1/2}{\sqrt{-c/b - 1/4}} - \arctan \frac{\varrho_{\rm d} - 1/2}{\sqrt{-c/b - 1/4}} = b\sqrt{-\frac{c}{b} - \frac{1}{4}}(L_2 + 1) \ . \tag{3.11}$$

It is not difficult to verify the following facts: as a function of $c \in [-\infty, -b/4]$ the left hand side of (3.11) is a monotonic function increasing from 0 to $-\pi$. Hence, (3.11) admits a unique solution in this case.

We can then conclude that in such a case the stationary Mean Field equation has the unique solution given by (3.10) with the constant c as in (3.11).

Case $1 \geq \varrho_u > \varrho_d > 1/2$. In this case, the left hand side of (3.11) tends to zero for $c \to -b/4$, so that (3.11) has a solution provided

$$\lim_{c \to -b/4} \frac{\arctan \dfrac{\varrho_{\rm u} - 1/2}{\sqrt{-c/b - 1/4}} - \arctan \dfrac{\varrho_{\rm d} - 1/2}{\sqrt{-c/b - 1/4}}}{b\sqrt{-\dfrac{c}{b} - \dfrac{1}{4}}(L_2 + 1)} > 1 \quad .$$

By computing the limit above, we get the condition

$$\frac{\varrho_{\rm u} - \varrho_{\rm d}}{b(L_2 + 1)(\varrho_{\rm u} - 1/2)(\varrho_{\rm d} - 1/2)} > 1 \quad . \tag{3.12}$$

We recall, now, that in this case it is also possible to find a solution of the Mean Field equation (3.7) with $0 > c > -b/4$. By a standard computation we find the solution

$$\varrho(z_2) = \frac{u_2 - u_1 \exp\{-bz_2(u_2 - u_1) - \log[(\varrho_{\rm u} - u_1)/(\varrho_{\rm u} - u_2]\}}{1 - \exp\{-bz_2(u_2 - u_1) - \log[(\varrho_{\rm u} - u_1)/(\varrho_{\rm u} - u_2]\}} \quad , \tag{3.13}$$

where

$$u_1 = \frac{1 - \sqrt{1 + 4c/b}}{2} < u_2 = \frac{1 + \sqrt{1 + 4c/b}}{2} \quad , \tag{3.14}$$

where the constant c, hidden in the expressions of u_1 and u_2, can be obtained by requiring $u(L_2 + 1) = \varrho_{\rm d}$, namely,

$$\varrho_{\rm d} = \frac{u_2 - u_1 \exp\{-b(L_2 + 1)(u_2 - u_1) - \log[(\varrho_{\rm u} - u_1)/(\varrho_{\rm u} - u_2]\}}{1 - \exp\{-b(L_2 + 1)(u_2 - u_1) - \log[(\varrho_{\rm u} - u_1)/(\varrho_{\rm u} - u_2]\}} \quad . \tag{3.15}$$

By computing the limit, for $c \to -b/4$ of the ratio on the right hand side of (3.15), it is possible to show that such a limit is either larger or smaller than $\varrho_{\rm d}$ if and only if the equality (3.12) is satisfied. This occurrence is related to the existence of solutions to (3.15). Hence, we have that the solution of the stationary Mean Field equation is given by (3.10) provided (3.12) is satisfied, otherwise it is given by (3.13).

3.2. Numerical verification of the Mean Field prediction

We now test numerically how accurate is the Mean Field prediction of the stationary density profile. To measure experimentally such a profile we proceed as follows. We chose two numbers $1 \ll t_{\rm term} \ll t_{\rm max}$ that are called, respectively, *thermalization* and *maximal* time. As an estimator for the density $\varrho(z_2)$ we use

$$\frac{1}{L_1} \frac{1}{t_{\rm max} - t_{\rm term} + 1} \sum_{s=t_{\rm term}+1}^{t_{\rm max}} \sum_{i=1}^{n(s)} \mathbb{I}_{\{x_2(i,s)=z_2\}} \quad , \tag{3.16}$$

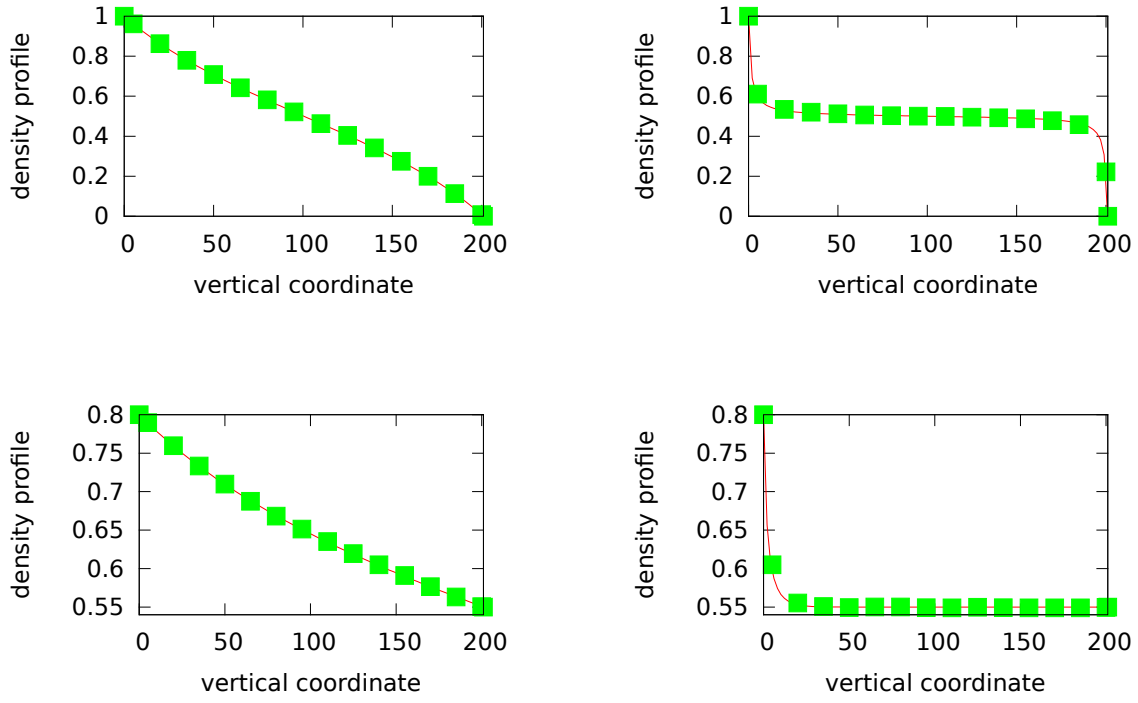

Figure 3.3: Density profiles. Comparison with numerical results (dots) and the Mean Field solution (solid lines). The cases described in Section 3.2 are considered: (i) top left, (ii) top right, (iii) bottom left, and (iv) bottom right.

where $\mathbb{I}_{\{\text{condition}\}}$ is equal to one if the condition is true and to zero otherwise.

The thermalization and maximal time are chosen *ad hoc* so that the measure is performed when the system is in the stationary state and so that the measure is sufficiently stable.

We choose the geometrical parameters $L_1 = 100$ and $L_2 = 200$ and the probabilistic one $h = 1/2$. Then we vary the remaining ones according to the following four cases:

(i) $\varrho_{\mathrm{u}} = 1$, $\varrho_{\mathrm{d}} = 0$, and $\delta = 0.008$: the mean field solution is given by (3.10) with $c = -0.007887$;

(ii) $\varrho_{\mathrm{u}} = 1$, $\varrho_{\mathrm{d}} = 0$, and $\delta = 0.8$: the mean field solution is given by (3.10) with $c = -0.400149$;

(iii) $\varrho_{\mathrm{u}} = 0.8$, $\varrho_{\mathrm{d}} = 0.55$, and $\delta = 0.008$: since the first term of inequality (3.12) is equal to 5.18242, the mean field solution is given by (3.10) with $c = -0.00478572$;

(iv) $\varrho_{\mathrm{u}} = 0.8$, $\varrho_{\mathrm{d}} = 0.55$, and $\delta = 0.8$: since the first term of inequality (3.12) is equal to 0.0518242, the mean field solution is given by (3.13) with $c = -0.396$.

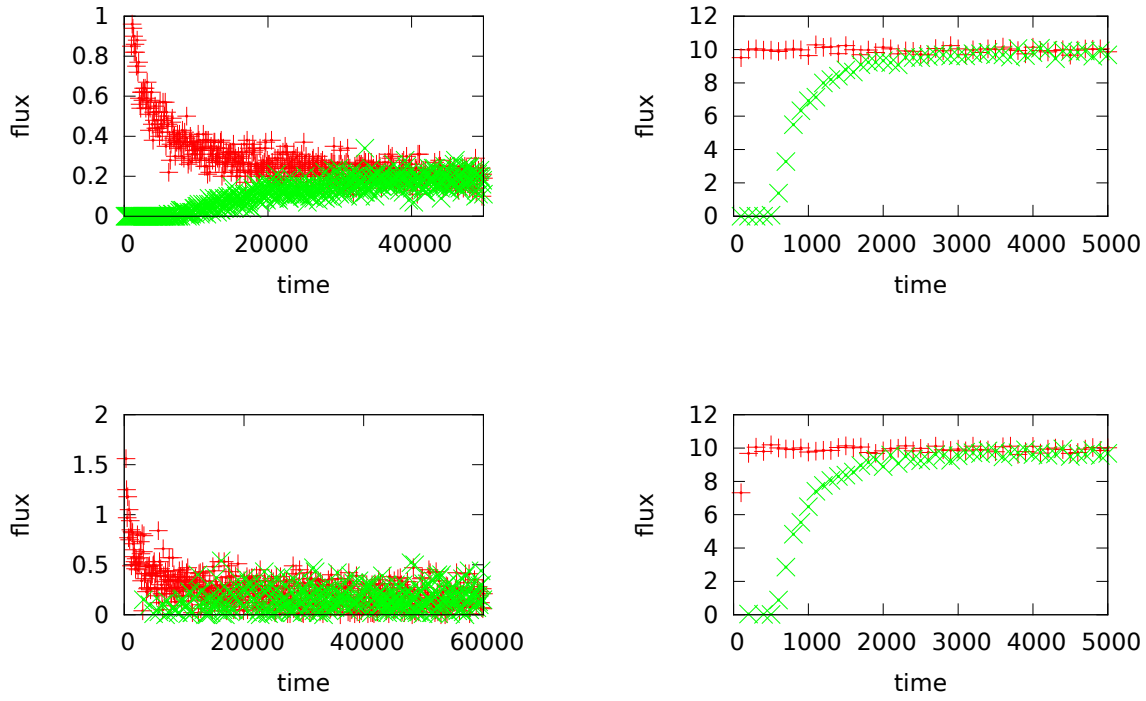

Figure 3.4: Numerical estimate of the ingoing (+) and outgoing (×) flux for the four cases described in Section 3.2: (i) top left, (ii) top right, (iii) bottom left, and (iv) bottom right.

The numerical simulations are performed with $t_{\text{term}} = 10^5$ and $t_{\max} = 5 \times 10^5$ and the corresponding results are depicted in Figure 3.3. In all the considered cases the match between the numerical data and the Mean Field prediction is strikingly good.

3.3. Thermalization time

Since the measuring of the density profile has to be performed in the stationary states, the choice of the thermalization time has to be done with care. One possibility to check if the system has reached stationarity is to compare the typical number of particles entering the system through the top boundary to that of the particles exiting from the bottom.

We proceed as following: to account for the number of particle crossing the top and bottom boundaries, we let $I(t)$ be the difference between the number of particles that entered at time t through the top boundary and that of the particles that exited through the same boundary. On the other hand, let $O(t)$ be the difference between the number of particles that exited at time t through the bottom boundary and that of the particles that entered through the same boundary. Both $I(t)$ and $O(t)$ are stochastic variables that can be positive or negative. We can expect that, if a stationary state is observed, in such a state $I(t)$ and

$O(t)$ will both fluctuate around the same value.

We also define two additional quantities: given the positive integer T, we let the *local ingoing and outgoing* fluxes at time t be as

$$F_T^{\rm i}(t) = \frac{1}{T} \sum_{s=\max\{0,t-T\}}^{t} I(s) \quad \text{and} \quad F_T^{\rm o}(t) = \frac{1}{T} \sum_{s=\max\{0,t-T\}}^{t} O(s) \ , \tag{3.17}$$

respectively.

In Figure 3.4 we plot the local ingoing and outgoing fluxes measured on the interval $T = 100$ for the four cases (i)–(iv) considered above. The data shown in the figures indicate the choice 10^5 for the thermalization time.

4. A biased birth and death model

The main physical problem we discuss in this paper is that of the typical time that (at stationarity) a particle spends in the strip before finding its way to go out. We refer to this time as the *residence time* and we will discuss its definition in detail in the next section.

Since from this point of view only vertical displacements are relevant, we can think to the "vertical" history of the particle as to the evolution of a non–homogeneous birth and death process for the vertical coordinate with a rule depending on the stationary density profile. In this section we recall general results on this birth and death model and in the next section we discuss how to apply such results to our 2D model. We mainly follow [6] for the general discussion. We derive explicit formulas in two specific simple cases, that will turn out to be very important from the physical point of view. For the sake of completeness we outline these computations in Subsections 4.1 and 4.2.

Let L be a positive integer, $[[0, L]] := \{0, 1, \dots, L\}$, and consider a random walk on $[[0, L]]$ with transition probabilities $p(x, y)$ with $x, y \in [[0, L]]$. We denote by $X_a(t)$, with $t = 0, 1, \dots$ the position of the walker at time t with initial position a. We assume that at each time the walker either does not move or moves to one of the neighboring sites, i.e., we assume $p(x, y) = 0$ for $x, y \in [[0, L]]$ such that $|x - y| \geq 2$. Moreover, we let $p_x = p(x, x + 1)$ with $x = 0, \dots, L-1$ be the probabilities to go to the right and $q_x = p(x, x-1)$ with $x = 1, \dots, L$ be the probabilities to go to the left. We assume $0 \leq p_{x-1} \leq q_x < 1$ for $x = 1, \dots, L$, namely, at each site the walker has the chance to go both to the left and to the right and the walk is left–biased. Furthermore, we assume that at least one of the "rest probabilities" $p(x, x) = 1 - (p_x + q_x)$ is different from zero so that the chain is aperiodic. We note that the more general situation in which the bias condition is removed can be treated as well, but for the sake of clarity, we consider the biased case.

In the case $0 < p_{x-1} \le q_x < 1$ for $x = 1, \dots, L$, since the birth and death process is aperiodic and positive recurrent, it has a unique invariant measure that can be written as

$$\pi(x) = \pi(0) \prod_{i=1}^{x} \frac{p_{i-1}}{q_i} \quad \text{for all } x = 1, \dots, L \ , \tag{4.18}$$

see [6, equation (4.1)]. Note that the proof of the above statement is immediate, since one just has to verify that the above measure satisfies the detailed balance equation $\pi(x)p(x, x+1) = \pi(x+1)p(x+1, x)$ for all $x = 1, \dots, L-1$.

In [6] the authors study in detail the properties of the first hitting time of the chain to any point of the lattice $[[0, L]]$ with any initial condition (initial position of the walker). We are interested only to the hitting time

$$T := \inf\{t \ge 1,\, X_L(t) = 0\} \ , \tag{4.19}$$

i.e., the random time that the walker started at L needs to reach the origin for the first time. The expectation of such a hitting time is given by

$$\mathbb{E}[T] = \sum_{i=1}^{L} \frac{1}{q_i \pi(i)} \sum_{j=i}^{L} \pi(j) = \frac{1}{q_L} + \sum_{i=1}^{L-1} \frac{1}{q_i} \Big(1 + \sum_{j=i+1}^{L} \prod_{k=i+1}^{j} \frac{p_{k-1}}{q_k} \Big) \ , \tag{4.20}$$

see [6, equation (4.3)].

The first very simple remark is that, since the velocity of the particle is bounded by one, the mean hitting time to 0 cannot be smaller than L. More precisely, by using (4.20) and recalling that $q_x < 1$ for $x = 1, \dots, L$ we get the ballistic lower bound

$$\mathbb{E}[T] \ge L \ . \tag{4.21}$$

A natural question is under which assumptions on the bias there exists a ballistic upper bound to the first hitting time to zero. We prove this bound in a very simple case, namely, when we assume that each bond is left–biased. More precisely, we show that if there exists $0 < \eta < 1$ such that $p_{x-1}/q_x \le \eta$ for $x = 1, \dots, L$, then

$$\mathbb{E}[T] \le \frac{L}{\underline{q}(1-\eta)} \tag{4.22}$$

where we have let $\underline{q} = \min\{q_1, \dots, q_L\}$. Indeed, from (4.20) we have that

$$\mathbb{E}[T] \le \frac{1}{\underline{q}} + \sum_{i=1}^{L-1} \frac{1}{\underline{q}} \Big(1 + \sum_{j=i+1}^{L} \prod_{k=i+1}^{j} \eta \Big) = \frac{1}{\underline{q}} + \frac{1}{\underline{q}} \sum_{i=1}^{L-1} \sum_{k=0}^{L-i} \eta^k \le \frac{1}{\underline{q}} + \frac{1}{\underline{q}} \sum_{i=1}^{L-1} \sum_{k=0}^{\infty} \eta^k$$

where we have omitted few simple steps. The statement (4.22) follows recalling that $\eta < 1$.

Finally, we remark that using equations (4.18) and (4.20) we can compute the expected value of the first hitting time T. In practice this is explicitly feasible only for some particularly easy choices of the probabilities p_x and q_x. In the next subsections we discuss two physically relevant cases.

4.1. Homogeneous case

Let $0 < p \leq q < 1$ be two real numbers and assume $p_x = p$ and $q_x = q$ for all $x = 0, \dots, L$. Note that this choice satisfies all the basic assumptions on the birth and death chain.

To compute the expected value of the first hitting time T it is convenient to set $\lambda = p/q$, so that, from (4.18), we have $\pi(x) = \pi(0)\lambda^x$. Equation (4.20) yields

$$\mathbb{E}[T] = \frac{1}{q}\sum_{i=1}^{L}\frac{1}{\lambda^i}\sum_{j=i}^{L}\lambda^j = \frac{1}{q}\sum_{i=1}^{L}\sum_{j=i}^{L}\lambda^{j-i} = \frac{1}{q}\sum_{i=1}^{L}\sum_{k=0}^{L-i}\lambda^k = \frac{1}{q(1-\lambda)}\sum_{i=1}^{L}(1-\lambda^{L-i+1}) \ .$$

By reordering the sum, we obtain

$$\mathbb{E}[T] = \frac{1}{q(1-\lambda)}\Big(L - \sum_{k=1}^{L}\lambda^k\Big) = \frac{1}{q(1-\lambda)}\Big(L+1-\frac{1-\lambda^{L+1}}{1-\lambda}\Big) = \frac{L}{q(1-\lambda)} - \frac{\lambda(1-\lambda^L)}{q(1-\lambda)^2} \ .$$

Recalling $\lambda = p/q$, we finally have the expression

$$\mathbb{E}[T] = \frac{L}{q-p} - \frac{p}{(q-p)^2}\Big[1-\Big(\frac{p}{q}\Big)^L\Big] \ . \tag{4.23}$$

A physical comment is useful: if $p/q < 1$, the behavior of the mean first hitting time on L is ballistic. On the other hand, we can prove that

$$\lim_{p\to q}\mathbb{E}[T] = \frac{L(L+1)}{2q}$$

Hence, in the symmetric limiting case the diffusive dependence of the mean hitting time on the length L is found. Note that the totally asymmetric limit $p \to 0$ will be considered in Section 4.3 and the ballistic scaling will be found.

4.2. A linear case

We now consider a case in which the transition probabilities q_x and p_x decrease linearly in the interval $[[0, L]]$. The physical interest of the peculiar choice we shall do will be clear in the next section. Let $A > 0$ and take

$$q_x = 2A + A(L-x) \quad \text{and} \quad p_x = A(L-x) \ . \tag{4.24}$$

By using (4.18) for the stationary measure, we find that

$$\pi(x) = \pi(0)\,\frac{L}{L+1}\,\frac{L-1}{L}\,\frac{L-2}{L-1}\,\cdots\cdots\,\frac{L-x+1}{L-x+2} = \pi(0)\,\frac{L-x+1}{L+1}\quad .$$

By (4.20), we get

$$\mathbb{E}[T] = \frac{1}{A}\sum_{i=1}^{L}\frac{1}{L+2-i}\,\frac{1}{L+1-i}\sum_{j=i}^{L}(L+1-j)\quad .$$

Since, it holds that

$$\sum_{j=i}^{L}(L+1-j) = \frac{1}{2}(L+2-i)(L-i+1)\quad ,$$

we finally get

$$\mathbb{E}[T] = \frac{L}{2A}\quad . \tag{4.25}$$

It is worth noting that, if A is a constant then the scaling is ballistic. But if A is small with L, then we can possibly expect to have a diffusive scaling.

4.3. The totally asymmetric case

A situation that will be useful in our discussion and that is not included in the results discussed above is the case $0 = p_{x-1} < q_x < 1$ for $x = 1, \dots, L$, which we refer as the *totally asymmetric* case. In such a case, by using the same strategy of proof as in [6], it is easy to show that

$$\mathbb{E}[T] = \sum_{i=1}^{L}\frac{1}{q_i}\quad . \tag{4.26}$$

The dependence of the mean hitting time to zero on the length of the system is, in this case, trivially ballistic. Indeed, from (4.26) we get the bounds

$$\mathbb{E}[T] \geq \frac{L}{\bar{q}}\quad \text{and}\quad \mathbb{E}[T] \leq \frac{L}{\underline{q}}\quad , \tag{4.27}$$

where we have set $\underline{q} = \min\{q_1, \dots, q_L\}$ and $\bar{q} = \max\{q_1, \dots, q_L\}$. Note that in the totally asymmetric homogeneous case, that is to say, $0 < q_x = q < 1$ for $x = 1, \dots, L$, we get $\mathbb{E}[T] = L/q$.

5. Residence time at stationarity

The main question we pose in this paper is to find estimates for the typical time spent by a particle in the strip before exiting through the bottom boundary.

To give a precise definition of such a time for the simple exclusion model on the strip defined in Section 2 we set $\varrho_{\rm u} = 1$ so that particles cannot exit the strip through the top boundary. Once the stationary state is reached, we look at the particles that enter from the top boundary and exit from the bottom one. We count after how many steps of the dynamics the particle exits from the bottom boundary and call *residence time* the average of such a time over all the particles entered in the system after the stationary state is reached. Note that, at each step of the dynamics, a number of particles equal to the number of particles in the system at the end of the preceding time step is tentatively moved.

Despite its evident physical interest, the residence time is quite a difficult object to treat mathematically. In this section we discuss a microscopic approach in which we follow the motion of a single particle in a stationary density profile that is treated as a fixed background. In Section 5.6 we shall treat the problem macroscopically, by using the Mean Field theory.

Recall that, at stationarity, the average density profile is given by a function that we have denoted by $\varrho(z_2)$. Making a thought experiment, imagine that a new particle is injected into the stationary system through the top boundary. To estimate the typical time this particle needs to find its way out through the bottom boundary we note that only vertical displacements are relevant. Moreover, we can think of the "vertical" history of the particle as to the evolution of the not homogeneous birth and death process defined in Section 4 with the peculiar choice of the jump probabilities p_x and q_x that will be discussed below. We let $L = L_2$ and imagine that the value $x = 0$ of the birth and death process represents the particle at the row $L_2 + 1$ of the lattice (bottom boundary), the value $x = L_2$ represents the particle at the row 1 of the lattice (the row close to the top boundary), and the generic value x represents the particle at the row $L_2 + 1 - x$ of the lattice. The only not zero transition probabilities of the birth and death process are chosen as

$$\begin{cases} q_x = \dfrac{1-h}{2}(1+\delta)[1-\varrho(L_2+1-x+1)] & \text{for } x = 1, \dots, L_2 \\ p_x = \dfrac{1-h}{2}(1-\delta)[1-\varrho(L_2+1-x-1)] & \text{for } x = 0, \dots, L_2 - 1 \end{cases} . \tag{5.28}$$

Indeed, recalling the expressions (3.2) for the probabilities u and d, the prefactor $(1-h)(1+\delta)/2$ in the expression of q_x is nothing but the probability d to move the particle in the real space downwards; while the second factor is nothing but the probability that, at stationarity, the site where the particle tries to jump is empty. The expression for p_x can be justified similarly. The rest probability $1 - (p_x + q_x)$ is nonzero as the particle can stay at the same site or perform a unit step in the horizontal direction.

We now propose a conjecture for the residence time of the exclusion model and we will test it numerically in the next section.

Analogy *The residence time*[1] *of the model introduced in Section 2 is equal to the mean value of the first hitting time to* 0 *for the birth and death process started at* L_2.

The main properties of birth and death processes have been recalled in Section 4. Those results and the conjecture based on the above analogy suggest that, for $\delta < 1$, the residence time is given by equation (4.20) where the stationary measure π is given by (4.18) with the jump probabilities p_i and q_i defined in (5.28). Since the stationary density profile is given with great accuracy by the stationary Mean Field equation, we can use these equations to give an estimate of the residence time of the model. It is worth noting that, since the expression of the stationary density profile is rather complicated, see (3.10) and (3.13), it will not be possible to derive in general explicit formulas for the residence time. On the other hand, since in (4.20) and (4.18) only finite product and sums are involved, we will be able to compute estimates for the residence time numerically for any values of the parameters of the model. In the case $\delta = 1$ the expression (4.26) should be used.

Let us now discuss three simple cases in which explicit expressions of the residence time can be derived explicitly.

5.1. Totally vertically asymmetric model

Recall we assumed $\varrho_{\mathrm{u}} = 1$. Consider, more, the case $\delta = 1$. From the profiles in Figure 3.3 (graphs on the right) it is rather clear that in this situation the density profile is with very good approximation constant throughout the strip.

Denote by $\bar{\varrho}$ such a constant value of the density profile. By (5.28), it follows that the birth and death model has the jump probabilities

$$q_x = (1-h)(1-\bar{\varrho}) \;\; x = 1, \dots, L_2 \quad \text{and} \quad p_x = 0 \;\; x = 0, \dots, L_2 - 1$$

Hence, by the results in Section 4.3, we have that the residence time is given by

$$R = \frac{L_2}{(1-h)(1-\bar{\varrho})} \;\; . \tag{5.29}$$

In particular, the large L_2 behavior of the residence time given by (5.29) is ballistic with a slope depending on the parameters h and $\bar{\varrho}$.

5.2. Large drift case

[1]Since in the real model a particle at the fictitious row $L_2 + 1$ cannot jump back to the real row L_2, one should set the probability $p(0,1) = 0$. This would be a problem for the birth and death process, where all the jumping probabilities has to be assumed strictly positive, but for our purpose it is not necessary, since we are only interested to the first hitting time to 0, so that when the 1D birth and death process reaches such a state it is stopped. Hence all our results will not depend on the choice of the probability $p(0,1)$.

Recall we assumed $\varrho_{\mathrm{u}} = 1$. Consider δ close to one. From the profiles in Figure 3.3 (graphs on the right) it is rather clear that in this situation the density profile is with very good approximation equal to a constant, denoted again by $\bar{\varrho}$. By (5.28) it follows that the birth and death model has the jump probabilities

$$q_x = \frac{1-h}{2}(1+\delta)(1-\bar{\varrho}) \;\; x = 1, \dots, L_2 \quad \text{and} \quad p_x = \frac{1-h}{2}(1-\delta)(1-\bar{\varrho}) \;\; x = 0, \dots, L_2 - 1$$

Hence, by (4.23), we have that the residence time is given by

$$R = \frac{L_2}{(1-h)(1-\bar{\varrho})\delta} - \frac{1-\delta}{2(1-h)(1-\bar{\varrho})\delta^2}\Big[1 - \Big(\frac{1-\delta}{1+\delta}\Big)^{L_2}\Big] \;\; . \tag{5.30}$$

The formula (5.30) suggests that in this case the dependence of the residence time on L_2 is ballistic, but this statement needs more care. Indeed, the equation above is based on the assumption that the density profile is constant with good approximation in this regime and such an assumption is based on the results obtained via the Mean Field equation. But we have to recall that the Mean Field equation has been (not rigorously) derived in the large volume limit with the drift parameter scaling to zero with L_2. For this reason it is not correct, in principle, to fix δ and let $L_2 \to \infty$ in the above formula.

We remark, that in this case we shall as well be able to deduce the ballistic scaling of the residence time with L_2 in Section 5.4 via a different argument.

5.3. Zero drift

Consider, now, the case $\delta = 0$ (zero drift) again for $\varrho_{\mathrm{u}} = 1$. In the absence of drift the stationary density profile is linear, hence

$$\varrho(z_2) = 1 - \frac{1-\varrho_{\mathrm{d}}}{L_2+1} z_2 \tag{5.31}$$

for $z_2 = 0, \dots, L_2 + 1$. By (5.28), we get also that

$$q_x = \frac{1-h}{2}\frac{1-\varrho_{\mathrm{d}}}{L_2+1}(L_2+2-x) \quad \text{and} \quad p_x = \frac{1-h}{2}\frac{1-\varrho_{\mathrm{d}}}{L_2+1}(L_2-x) \;\; .$$

Thus, by using the result (4.25) from Section 4.2, we find the residence time

$$R = \frac{L_2(L_2+1)}{(1-h)(1-\varrho_{\mathrm{d}})} \;\; . \tag{5.32}$$

As expected, the large volume ($L_2 \to \infty$) behavior of the residence time is quadratic in the purely diffusive zero drift case.

5.4. Dependence of the residence time on the length of the strip

In this section we focus on the dependence of the residence time on the length L_2 of the strip. We expect that for $\delta > 0$, since there is a preferred direction in the movement, the particles will have a not zero average vertical velocity. As a consequence, we expect a ballistic behavior and a linear dependence of the residence time on L_2.

We have already shown in Section 5.1 that this is indeed the case for $\delta = 1$. Assume, now, that the drift δ is fixed and $0 < \delta < 1$. From (5.28), we see

$$\frac{p_{x-1}}{q_x} = \frac{1-\delta}{1+\delta}\frac{1-\varrho(L_2+1-x)}{1-\varrho(L_2+1-x+1)}$$

for any $x = 1, \dots, L_2$. Since, $\varrho_{\mathrm{u}} = 1 > \varrho_{\mathrm{d}} \geq 0$ we can reasonably assume that the density profile is a decreasing function of the vertical spatial coordinate. Thus, $\varrho(L_2+1-x) > \varrho(L_2+1-x+1)$ implies that there exists $\eta < 1$ such that $p_{x-1}/q_x \leq \eta$. This remark and (4.22) ensure that, for any positive finite δ, the residence time has a ballistic dependence on the length of the strip.

Finally, for $\delta = 0$ we have shown in Section 5.3, cf. (5.32), that the residence time is quadratic in L_2 (diffusive scaling). We stress that this result is not trivial at all. Indeed, even in the case $\delta = 0$ the birth and death model that we use to investigate the property of the residence time is not symmetric. The lack of symmetry is due to

$$q_x - p_{x-1} = \frac{1-h}{2}\,\frac{1-\varrho_{\mathrm{d}}}{L_2+1}$$

for any $x = 1, \dots, L_2$. The diffusive scaling is a consequence of the fact that this difference vanishes as $1/(L_2+1)$.

5.5. Single file regime

The model we study is two-dimensional. Particles move in a strip from the top boundary towards the bottom one due to the presence of a drift δ or just because of a vertical biased diffusion due to the difference between the boundary densities on the top and on the bottom end of the strip. The particles are subjected also to horizontal displacements whose probability is controlled by the parameter h.

In the particular case $h = 0$, our model becomes 1D and particles move, each on its vertical line, as in a single file system. In other words in this case our model reduces to the 1D simple exclusion model with open boundaries. The specification "open boundaries" means that the system is finite and at the boundaries there is a rule prescribing the rate at which particles can either enter or leave the system.

This model has been widely studied, see for instance [14] for the seminal paper where the model was solved exactly in the totally asymmetric case. See, also, [9] for a general review.

Our results can be compared easily to those in [14] which refer to the totally asymmetric case, namely, for our case $\delta = 1$. In [14] one computes the stationary current J, namely, the net number of particles that for unit of time crosses one bond at stationarity. With our notation one finds

$$J = \begin{cases} 1/4 & \text{for } \varrho_{\rm d} \le 1/2 \\ \varrho_{\rm d}(1-\varrho_{\rm d}) & \text{for } \varrho_{\rm d} > 1/2 \end{cases} \tag{5.33}$$

in the case $\varrho_{\rm u} = 1$ (see [14, equations (58) and (60)]).

Now, since in the totally asymmetric case the stationary density throughout the system is equal to a constant $\bar\varrho$, we can write $J \approx \bar\varrho L_2/R$. Hence, we have that

$$R \approx \bar\varrho\, \frac{L_2}{J}$$

which reduces to our result (5.29) with $h = 0$ once we use (5.33) and notice that $\bar\varrho = 1/2$ for $\varrho_{\rm d} \le 1/2$ and $\bar\varrho = \varrho_{\rm d}$ for $\varrho_{\rm d} > 1/2$.

Additionally, we mention here an interesting result which is valid for the symmetric simple exclusion model in 1D on the whole line (no boundary). In both [19] and [17], the authors compute the variance of the position of a tagged particle and they prove that it is proportional to the square root of time, meaning that the typical distance spanned by the (symmetric) walker is proportional to $t^{1/4}$. In our problem we do not find any L_2^4 scaling for the residence time even in the single–file regime. Indeed, we think that there is no direct connection between the two problems. One important point is that the results in [17, 19] deal with a simple exclusion model without drift (symmetric) and without boundaries. In our problem, even in the zero drift ($\delta = 0$) case, a net flux is present due to the boundary conditions.

5.6. Mean Field approximation for the residence time

In this section we approach the residence time computation from a macroscopic point of view. In the Mean Field approximation the evolution of the systems can be described in terms of the density profile $m_t(z_1, z_2)$ evolving according to the Partial Differential Equation (3.6). Such an equation can be tought of as a continuity equation for the current two–dimensional vector

$$\vec J_t = -\frac{1}{2} h \frac{\partial m_t}{\partial z_1}\vec e_1 + \Big(-\frac{1}{2}(1-h)\frac{\partial m_t}{\partial z_2} + \delta(1-h) m_t(1-m_t)\Big)\vec e_2$$

where $\vec e_1$ and $\vec e_2$ are the unitary vectors of the lattice.

At stationarity, the density profile $\varrho(z_2)$ does not depend on the horizontal coordinate, so that the current is parallel to the vertical direction and its intensity is given by

$$J = -\frac{1}{2}(1-h)\frac{\partial \varrho}{\partial z_2}(z_2) + \delta(1-h)\varrho(z_2)[1-\varrho(z_2)] = -\frac{1}{2}(1-h)\varrho'(0) \tag{5.34}$$

where we have used (3.7), (3.9), and the fact that $\varrho_{\mathrm{u}} = 1$. Note that $-2J/(1-h)$ is the constant c appearing in equation (3.9).

As we have already done in Section 5.5, we can relate the stationary current to the residence time. Indeed, in the Mean Field (continuous space and time) model the stationary velocity of a particle $v(z_2)$ is such that $\varrho(z_2)v(z_2) = J$. Then, an easy integration gives

$$R = \int_0^{L_2+1} \frac{\varrho(z_2)}{J}\,\mathrm{d}z_2 = -\frac{2}{(1-h)\varrho'(0)} \int_0^{L_2+1} \varrho(z_2)\,\mathrm{d}z_2 \tag{5.35}$$

In the next section we shall compare this Mean Field prediction of the residence time with the numerical results.

For finite values of the length, we cannot use the above equation to write an explicit expression of the residence time in terms of the parameter of the model, indeed $\varrho'(0)$ is nothing but the constant c in equation (3.9) (recall $\varrho_{\mathrm{u}} = 1$) which is, in turn, the solution of either the equation (3.11) or (3.15).

On the other hand it is possible to write a nice parametric representation of the residence time in terms of J. Indeed, by using (3.9) and recalling $c = -2J/(1-h)$ we get

$$L_2 + 1 = \int_1^{\varrho_{\mathrm{d}}} \frac{\mathrm{d}\varrho}{2\delta\varrho(1-\varrho) - 2J/(1-h)} \tag{5.36}$$

Moreover, by performing the change of variables $z_2 \to \varrho(z_2)$ in (5.35) and using again (3.9) we get

$$R = \int_0^{L_2+1} \frac{\varrho(z_2)}{J}\,\mathrm{d}z_2 = \frac{1}{J}\int_1^{\varrho_{\mathrm{d}}} \frac{\varrho}{\varrho'}\,\mathrm{d}\varrho = \frac{1}{J}\int_1^{\varrho_{\mathrm{d}}} \frac{\varrho}{2\delta\varrho(1-\varrho) - 2J/(1-h)}\,\mathrm{d}\varrho \tag{5.37}$$

Note, finally that (5.36) and (5.37) provide a nice parametric representation of the residence time R in terms of the parameter J.

We show, now, how we can use the above representation of the residence time to find explicit formula in some asymptotic cases. For instance in the case δ close to 1, we know that the density profile is approximatevely equal to a constant $\bar{\varrho}$. In this case, then, by (5.36) and (5.37) we get

$$L_2 + 1 = \frac{\varrho_{\mathrm{d}} - 1}{2\delta\bar{\varrho}(1-\bar{\varrho}) - 2J/(1-h)} \quad \text{and} \quad R = \frac{1}{J}\frac{\varrho_{\mathrm{d}} - 1}{2\delta\bar{\varrho}(1-\bar{\varrho}) - 2J/(1-h)}\bar{\varrho}$$

which implies

$$R = \frac{1}{J}\bar{\varrho}(L_2+1) \approx \frac{1}{\delta(1-\bar{\varrho})(1-h)}L_2 \tag{5.38}$$

for L_2 large. Note that the Mean Field result is close to the first term obtained in (5.30) by means of the birth and death model.

On the other hand, in the zero drift $\delta = 0$ case we have that (5.36) and (5.37) reduce to the equalities

$$L_2 + 1 = \frac{1-h}{2J}(1-\varrho_{\rm d}) \quad \text{and} \quad R = \frac{1-h}{4J^2}(1-\varrho_{\rm d}^2)$$

which imply

$$R = \frac{1}{(1-h)}\frac{1+\varrho_{\rm d}}{1-\varrho_{\rm d}}(L_2+1)^2. \tag{5.39}$$

This formula has to be compared to the prediction (5.32) for the residence time in the zero drift case obtained in the framework of the birth and death model approximation.

The mean field residence time expression (5.39) can be considered the residence time according to the birth and death model corrected by a term proportional to $\varrho_{\rm d}/(1-\varrho_{\rm d})$. When $\varrho_{\rm d}$ is zero both expressions are the same. The correction can be understood is due to the correlated motion in the one dimensional bouncing back case. Using renormalisation techniques, Fedders [19] found that the diffusion constant has to be corrected by a similar term in the stationary case. We will see that expression (5.39) only agrees well the Monte Carlo simulations as long as $h = 0$.

6. Numerical estimates of the residence time

In this section we test numerically the validity of the analytic computations developed in Section 5. We choose the parameters of the model as follows: take $\varrho_{\rm u} = 1$, $L_1 = 100$, and consider the cases

$$L_2 = 100, 200, \quad \delta = 0, 0.2, 0.4, 0.6, 0.8, 1, \quad \varrho_{\rm d} = 0, 0.4, 0.8, \quad h = 0, 0.4, 0.8.$$

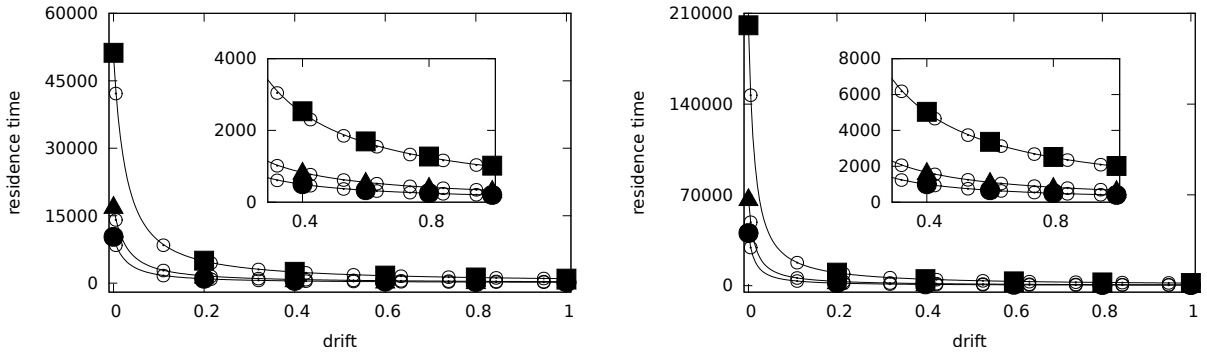

Figure 6.5: Residence time versus drift in the cases $\varrho_{\rm d} = 0$ and $L_2 = 100$ (left) and $L_2 = 200$ (right). The symbols •, ▲, and ■ refer, respectively, to the cases $h = 0, 0.4, 0.8$. The inset in the left picture is just a zoom of part of the data of the same picture. Solid lines are the birth and death theoretical prediction. Open circles are the Mean Field theoretical prediction (5.35).

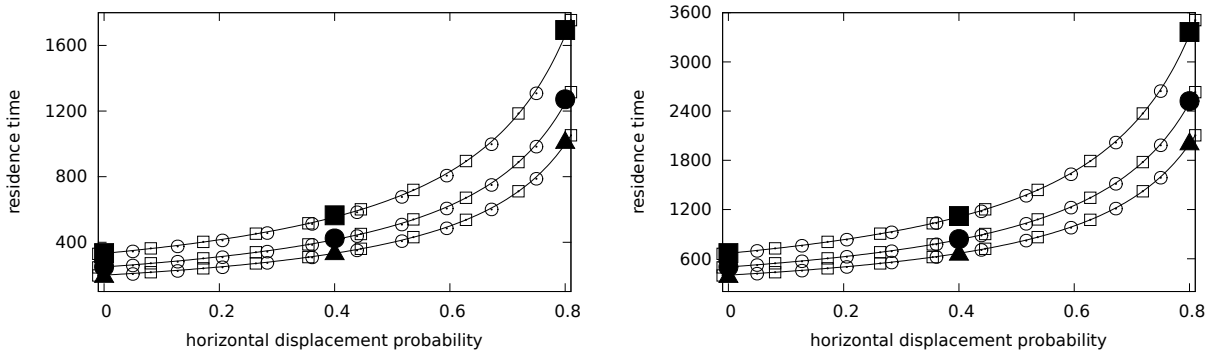

Figure 6.6: Residence time versus the horizontal displacement probability h in the cases $\varrho_{\rm d} = 0$ and $L_2 = 100$ (left) and $L_2 = 200$ (right). The symbols ■, •, and ▲ refer, respectively, to the cases $\delta = 0.6, 0.8, 1$. Solid lines are the birth and death theoretical prediction. Open squares are the approximated theoretical prediction (5.30) with $\bar{\varrho} = 1/2$, which is valid in the large drift regime. Open circles are the Mean Field theoretical prediction (5.35).

In all these cases, the residence time has been evaluated by averaging over all the particles entered in the system through the top boundary after the time $t_{\rm term}$, namely, at stationarity, and exited through the bottom one at a time smaller than $t_{\rm max}$. The simulations have been performed with $t_{\rm term} = 5 \times 10^5$ and $t_{\rm max} = 5 \times 10^6$.

To check the dependence of the residence time on the length of the strip we had to consider a few more cases with larger L_2, viz. $L_2 = 300, 400$. In these cases, due to the length of the strip, we had to use $t_{\rm term} = 10^6$ and increase $t_{\rm max}$ up to 4×10^7 in the more delicate situations ($h = 0.8$). It is important to note that in the cases $L_2 = 300, 400$ and $\varrho_{\rm d} = 0.8$, the initial configuration of the system has been chosen by populating the system by putting particles with probability 0.95. Indeed, by starting the system with all the sites empty, the dynamics was trapped in a sort of "meta–stationary" state with density approximatively constant and slightly larger than 0.8.

In all the pictures the vertical bar representing the statistical error is not visible since it is smaller than the symbol representing the measured value of the residence time.

We compare the numerical results with the theoretical predictions based both on the birth and death analogy and on the Mean Field approach. In general the birth and death theoretical prediction of the residence time is the value given by (4.20) with the stationary measure π given by (4.18) where the jump probabilities p_i and q_i are defined in (5.28). Since we could not derive explicit expressions in terms of the model parameters, the birth and death theoretical prediction has been computed by performing sums and products numerically. In the case $\delta = 1$ (see, the discussion in Section 6.2) the birth and death theoretical prediction is the value given by (4.26) with the q_i's defined in (5.28). In the case $\delta = 0$ (see for instance

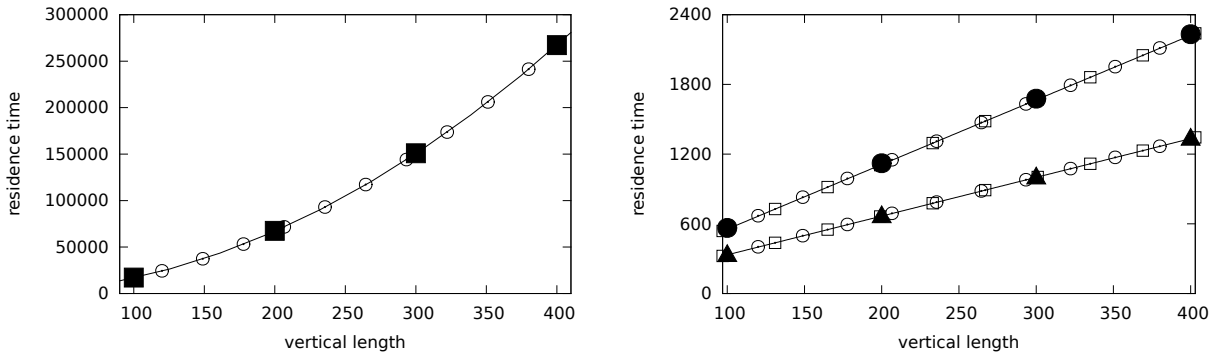

Figure 6.7: Residence time versus length of the strip L_2 in the case $\varrho_{\rm d} = 0$ and $h = 0.4$. The symbol ■ refers to the case $\delta = 0$ (left picture) while the symbols • and ▲ refer, respectively, to the cases $\delta = 0.6, 1$. Solid lines are the theoretical prediction based on the birth and death model; in the picture in the left the explicit expression (5.32) is used, Open squares are the approximated theoretical prediction (5.30) with $\bar{\varrho} = 1/2$, which is valid in the large drift regime. Open circles are the Mean Field theoretical prediction (5.35).

the discussion in Section 6.3) the theoretical prediction is given explicitly by (5.32).

We find that the match between the theoretical predictions based both on the birth and death analogy and on the Mean Field approach and the numerical data is perfect for any choice of the parameters of the model provided either $\varrho_{\rm d} = 0$ or $\delta = 1$ (or both). To illustrate this fact we first discuss our data at $\varrho_{\rm d} = 0$ and let $h = 0, 0.4, 0.8$ and $\delta = 0, 0.2, 0.4, 0.6, 0.8, 1$. Then, we consider $\delta = 1$ and let $h = 0, 0.4, 0.8$ and $\varrho_{\rm d} = 0, 0.4, 0.8$.

Finally, for the region where the match between the theoretical predictions and the numerical results is not good, we consider the worst case from the point of view of drift, namely, we choose $\delta = 0$ and let, again, $h = 0, 0.4, 0.8$ and $\varrho_{\rm d} = 0, 0.4, 0.8$. We shall notice that the match between theory and experiment, even if qualitatively correct, it becomes progressively worse with increasing $\varrho_{\rm d}$.

6.1. Case $\varrho_{\rm d} = 0$

We discuss first the case $\varrho_{\rm d} = 0$ and show that here the theoretical predictions of the residence time based on both the birth and death analogy and the Mean Field computation discussed in Section 5 agree perfectly with the numerical results.

In Figure 6.5 it is shown the dependence of the residence time on the drift δ for $\varrho_{\rm d} = 0$ and for different values of the horizontal displacement probability h. The dependence of the residence time on the horizontal displacement probability for different values of the drift is shown in Figure 6.6.

The fact that the residence time decreases with the drift and increases with the horizontal displacement probability is completely reasonable. The match between the simulation data

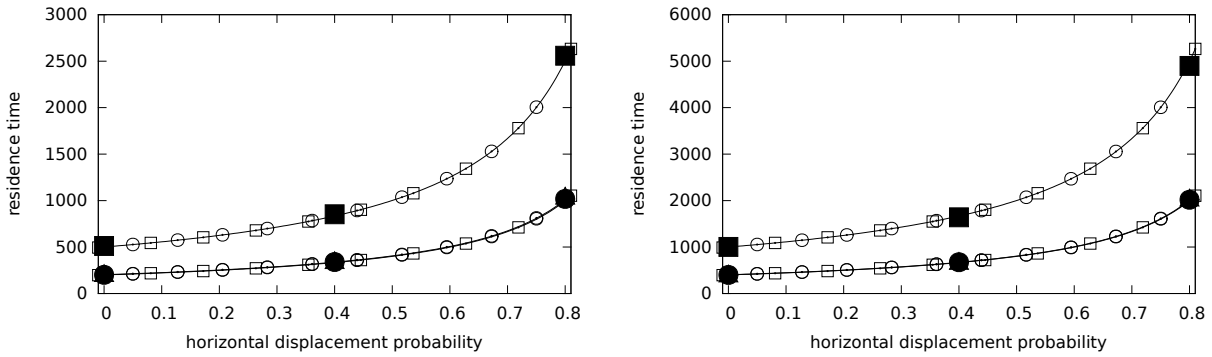

Figure 6.8: Residence time versus the horizontal displacement probability h in the cases $\delta = 1$ and $L_2 = 100$ (left) and $L_2 = 200$ (right). The symbols •, ▲, and ■ refer, respectively, to the cases $\varrho_{\rm d} = 0, 0.4, 0.8$. Note that bullets and black triangle are perfectly coinciding, this is due to the fact that in this regime the residence time does not depend that much on the bottom boundary density, provided it is smaller that 1/2. In such a case, indeed, the density profile inside the strip is almost perfectly constant and equal to 1/2. Solid lines are the theoretical prediction based on the birth and death model. Open squares are the approximated theoretical prediction (5.30) valid in the large drift regime with $\bar\varrho = 1/2$ for the cases $\varrho_{\rm d} = 0, 0.4$ and with $\bar\varrho = 8/10$ in the case $\varrho_{\rm d} = 0.8$. Indeed, in the first two cases the density profile is almost constantly equal to 1/2, while in the last case it is almost constantly equal to 8/10. Open circles are the Mean Field theoretical prediction (5.35).

and the theoretical predictions is perfect. It is remarkable the fact that even the approximated expression (5.30) (which in the case $\delta = 1$ reduces to (5.29)) gives a perfect estimate of the residence time. This is due to the fact that for the values of the parameter that we have chosen the stationary density profile throughout the system is constantly equal to 1/2 with very a good approximation.

In Figure 6.7, the residence time in the case $\varrho_{\rm d}$ has been plotted as a function of the length L_2 of the strip for different values of the drift and for $h = 0.4$. It is remarkable to note the striking match between theory and simulation. In particular the fact that the behavior is linear (ballistic) for $\delta > 0$ and quadratic (diffusive) for $\delta = 0$, see the theoretical discussion in Section 5.4, is confirmed by the numerical experiment.

6.2. Case $\delta = 1$

This is the case of totally asymmetric simple exclusion rule along the vertical direction. Here, particles can never jump upwards. We show that, for this scenario, the theoretical predictions of the residence time based on both the birth and death analogy and the Mean Field computation discussed in Section 5 agree perfectly with the numerical results.

We show three pictures: the dependence of the residence time on the horizontal dis-

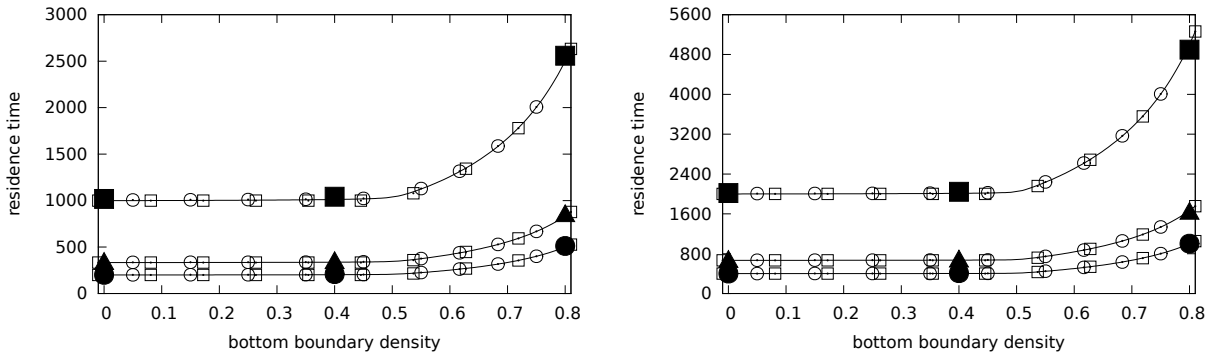

Figure 6.9: Residence time versus the bottom boundary density $\varrho_{\rm d}$ in the cases $\delta = 1$ and $L_2 = 100$ (left) and $L_2 = 200$ (right). The symbols •, ▲, and ■ refer, respectively, to the cases $h = 0, 0.4, 0.8$. Solid lines are the theoretical prediction based on the birth and death model. Open squares are the approximated theoretical prediction (5.30) valid in the large drift regime with $\bar\varrho = 1/2$ for $\varrho_{\rm d} \le 1/2$ and with $\bar\varrho = \varrho_{\rm d}$ for $\varrho_{\rm d} > 1/2$. Indeed, when $\varrho_{\rm d} < 1/2$ the density profile is almost constantly equal to $1/2$, while for $\varrho_{\rm d} > 1/2$ it is almost constantly equal to $\varrho_{\rm d}$. Open circles are the Mean Field theoretical prediction (5.35).

placement probability h (Figure 6.8), the dependence on the bottom boundary density $\varrho_{\rm d}$ (Figure 6.9), and, finally, the dependence on the length of the strip L_2 (Figure 6.10).

We do not repeat the discussion in detail. We just mention that the linearity of the residence time with respect to the length of the strip is confirmed by the experimental data and refer the reader to the caption of the pictures for more specific comments.

6.3. Case $\delta = 0$

We discuss now the case of a symmetric simple exclusion rule along the vertical direction. As we already mentioned at the beginning of this section, in this case the match between the theoretical prediction and the numerical data is only qualitatively good and quantitavely worst when $\varrho_{\rm d}$ is increased.

We also remark that, fixed $\varrho_{\rm d}$, the match with the prediction based on the birth and death analogy is better at larger values of the horizontal displacement probability h. On the other hand, fixed $\varrho_{\rm d}$, the match with the Mean Field prediction is better at smaller values of the horizontal displacement probability h and perfect at $h = 0$.

The physical interpretation of this fact is that at large $\varrho_{\rm d}$ particles accumulate at the bottom exit and, due to bouncing back of particles, fluctuations are not more negligible. For this reason our theoretical predictions, which are based only on the stationary shape of the density profile, are not anymore always efficient. We shall discuss this point also in Section 6.4.

We show three pictures: the dependence of the residence time on the horizontal dis-

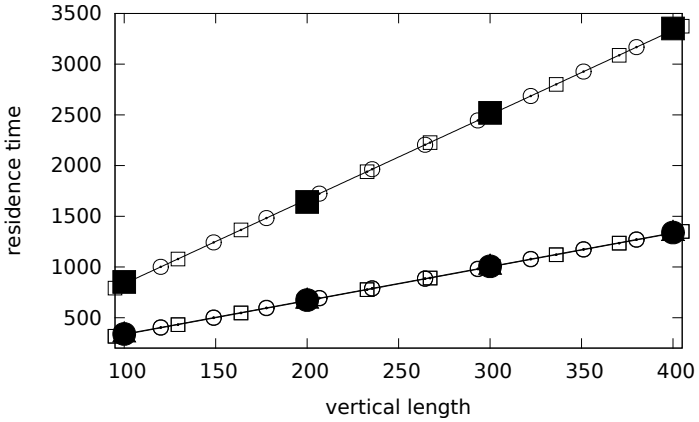

Figure 6.10: Residence time versus the vertical length of the strip L_2 in the case $\delta = 1$ and $h = 0.4$. The symbols •, ▲, and ■ refer, respectively, to the cases $\varrho_{\rm d} = 0, 0.4, 0.8$. Note that bullets and black triangle are perfectly coinciding, this is due to the fact that in this regime the residence time does not depend that much on the bottom boundary density, provided it is smaller that $1/2$. In such a case, indeed, the density profile inside the strip is almost perfectly constant and equal to $1/2$. Solid lines are the theoretical prediction based on the birth and death model. Open squares are the approximated theoretical prediction (5.30) valid in the large drift regime with $\bar{\varrho} = 1/2$ for the cases $\varrho_{\rm d} = 0, 0.4$ and with $\bar{\varrho} = 8/10$ in the case $\varrho_{\rm d} = 0.8$. Indeed, in the first two cases the density profile is almost constantly equal to $1/2$, while in the last case it is almost constantly equal to $8/10$. Open circles are the Mean Field theoretical prediction (5.35).

placement probability h (Figure 6.11), the dependence on the bottom boundary density $\varrho_{\rm d}$ (Figure 6.12), and, finally, the dependence on the length of the strip L_2 (Figure 6.13).

Note that in this section, since $\delta = 0$, the theoretical prediction based on the birth and death analogy is given by the explicit formula (5.32), whereas the Mean Field prediction is (5.39).

The relevant comment now, see Figures 6.11, 6.13, and 6.14, is that the match between the Mean Field prediction and the experiment is perfect at $h = 0$, whereas it gets worst when h is increased. On the other hand, the birth and death analogy poorly predicts the residence time behavior $h = 0$, whereas it captures the phenomenon better when h is increased. This phenomenon can be explained via two mechanisms: bouncing back and the possibility to bypass clusters of blocking particles. The former suggests that fluctuations become important in this regime so that a model based only on the average stationary density profile cannot explain the behavior of the system. On the other hand, the latter phenomenon suggests that the effect of bouncing back is milder when the horizontal displacement probability is larger, since particles have a good chance to avoid blocking clusters.

It is interesting to remark that the Mean Field expression (5.39) for the case $\delta = 0$, and L_2 large, is given by the expression (5.32) predicted by the birth and death analogy plus a

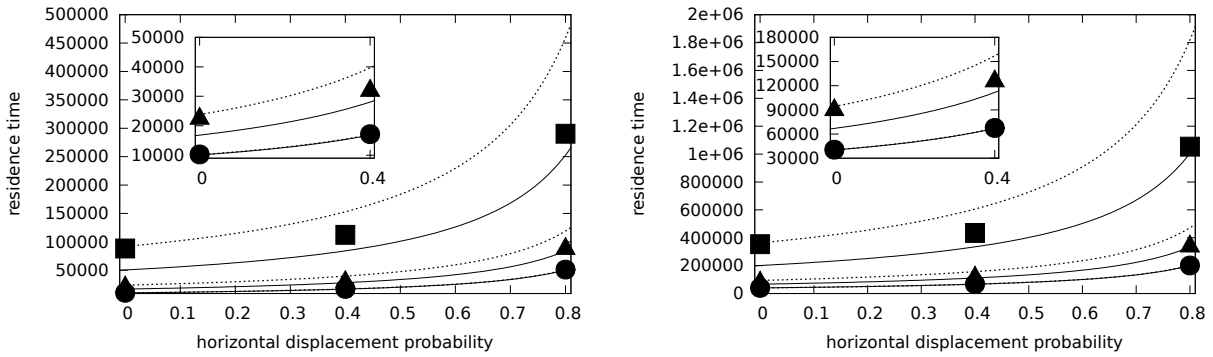

Figure 6.11: Residence time versus the horizontal displacement probability h in the cases $\delta = 0$ and $L_2 = 100$ (left) and $L_2 = 200$ (right). The symbols •, ▲, and ■ refer, respectively, to the cases $\varrho_{\rm d} = 0, 0.4, 0.8$. Solid lines are the theoretical prediction (5.32) from the bottom to the top for the cases $\varrho_{\rm d} = 0, 0.4, 0.8$. Dotted lines are the Mean Field prediction (5.39) from the bottom to the top for the cases $\varrho_{\rm d} = 0, 0.4, 0.8$. The dotted and the solid lines corresponding to the case $\varrho_{\rm d} = 0$ cannot be distinguished in the picture. The insets are just a zoom of part of the data of the same picture.

term that can be ascribed the two point correlations, see [19]. We could then guess that the correct expression of the residence time could be the birth and death prediction plus the two point correlation contribution weighted by a function depending on h tending to 1 for $h \to 0$ and to 0 for $h \to 1$.

6.4. Non–monotonic behavior in the bouncing back regime

As it has been seen in the previous section the residence time is typically an increasing function of the horizontal displacement probability. This is an obvious fact. Indeed, when h is increased particles spend a lot of time in performing horizontal jumps which are a waste of time in the run towards the bottom exit.

In this section we show that in the regime in which the bouncing back phenomenon is present a small not zero horizontal probability displacement can favour the exit of the particles.

We have performed the following simulations: $\varrho_{\rm u} = 1$ (as always), $L_1 = 100$, $L_2 = 200$, $\delta = 0$,

$$\varrho_{\rm d} = 0, 0.05, \ldots, 0.5, 0.6, 0.7, 0.8, \qquad \text{and} \qquad h = 0, 0.005, 0.010, \ldots, 0.125 \ .$$

As before, in all these cases, the residence time has been evaluated by averaging over all the particles entered in the system through the top boundary after the time $t_{\rm term}$, namely, at stationarity, and exited through the bottom one at a time smaller than $t_{\rm max}$. The simulations have been performed with $t_{\rm term} = 1 \times 10^6$ and $t_{\rm max} = 1 \times 10^7$.

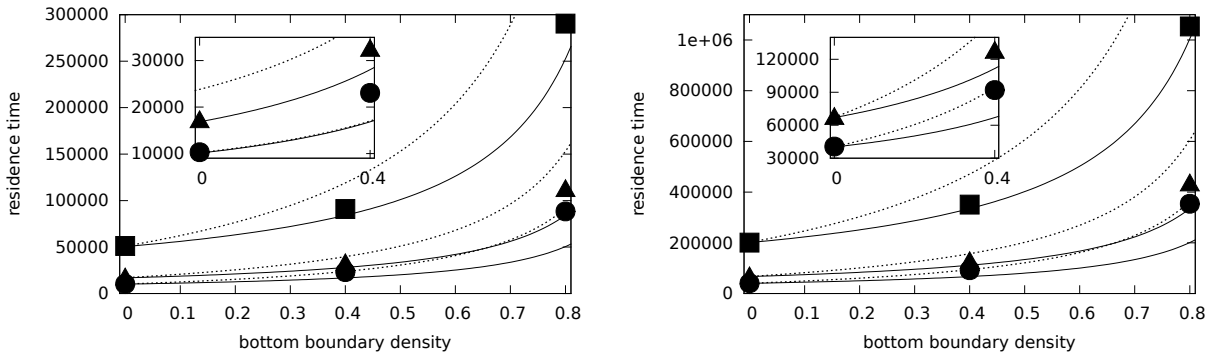

Figure 6.12: Residence time versus the bottom boundary density $\varrho_{\rm d}$ in the cases $\delta = 0$ and $L_2 = 100$ (left) and $L_2 = 200$ (right). The symbols •, ▲, and ■ refer, respectively, to the cases $h = 0, 0.4, 0.8$. Solid lines are the theoretical prediction (5.32) from the bottom to the top for the cases $h = 0, 0.4, 0.8$. Dotted lines are the Mean Field prediction (5.39) from the bottom to the top for the cases $h = 0, 0.4, 0.8$. The insets are just a zoom of part of the data of the same picture.

In Figure 6.15, the residence time is plotted as function of the horizontal displacement probability. It is remarkable the presence of a minimum at small values of h. This fact can be interpreted as follows: in the bouncing back regime, namely, when $\varrho_{\rm d}$ is high and δ low, a particle can find a blocking cluster of particles in its way out through the bottom boundary. In such a situation, then, having a larger horizontal displacement probability can help the particle to bypass the obstacle. Obviously, if h is increased too much this effect disappears due to the time wasted by the particles in horizontal movements. A similar non-monotonicity effect has been noticed in [10], for a scenario refereeing to the motion of self-propelled particles in heterogeneous environments. The role of our parameter h is played there by a noise indicator.

7. Conclusions

We focused our attention on the study of the simplest 2D model that mimics the flow of particles in a straight strip under the effect of different driving boundary conditions and external fields. We studied the residence time, i.e., the typical time a particle entering the strip at stationarity from the top boundary needs to exit through the bottom one, under the assumption that particles in the strip interact only via hard–core exclusion and vertical boundaries are reflecting.

We explored the dependence of the residence time on the external driving force, length of the strip, horizontal diffusion, and boundary conditions. We have shown that, in almost all the considered regimes, the mean residence time is equal to the average time needed to cross the strip by a particle performing a random walk in a background prescribed by the

stationary density profile of the original model. In this way, in particular, we recover the structure of the fluxes as well as the residence times proven mathematically in 1D in [14].

A completely macroscopic point of view has also been alternatively adopted, i.e. a Mean Field computation of the residence time has been performed by connecting such a quantity to the stationary current in the system. It has been shown that also this point of view porvides very satisfactory results.

This picture fails to be correct in the case in which there is a particle accumulation close to the bottom boundary (exit). In this regime, we discover new effects that are consequence of the two–dimensionality of the system. The most relevant is the non–monotonic behavior in changes in the horizontal displacement probability in the bouncing back regime.

A second very interesting result is the fact that in this bouncing back regime the Mean Field approach gives a very good prediction of the residence time in the single file (zero horizontal displacement probability) case. On the other hand, if the horizontal displacement probability is large (close to one) the Mean Field prediction is poor and the one based on the analogy with the birth and death model on the background of the stationary density profile yield a very good prediction. The comparison between the two theoretical models in the zero drift case is summarized in figure 7.16 in which the difference (normalized with respect to the Monte Carlo measure) between the theoretical predictions and the Monte Carlo residence time measure is plotted as a function of δ and ϱ_{d} in the case $L_2 = 100$ for different values of the horizontal displacement probability.

This particle accumulation situation can be realized artificially by inserting obstacles in the strip. We then expect interesting non–linear phenomena to show up. We shall study this regime in a follow–up paper.

Acknowledgements
ENMC thanks ICMS (TU/e, Eindhoven, The Netherlands) for the very kind hospitality and for finacial support.

The authors appreciate funding of the Royal Dutch Academy of Sciences programme "Over grenzen" for travel support.

The authors thank Kerry Landman (Melbourne), Roberto Fernández (Utrecht), and Lorenzo Bertini (Roma) for very stimulating discussions and useful references. The authors also thank an anonymous referee for having suggested to compare the residence time estimates to Mean Field predictions and for having suggested the parametric representation of residence time exploited in Section 5.6.

References

[1] A. Ahrony, D. Stauffer, "Introduction to Percolation Theory." Taylor and Francis, 1994.

[2] D. Andreucci, D. Bellaveglia, E.N.M. Cirillo, "A model for enhanced and selective transport through biological membranes with alternating pores." *Mathematical Biosciences* **257**, 42–49 (2014).

[3] D. Andreucci, D. Bellaveglia, E.N.M. Cirillo, S. Marconi, "Effect of intracellular diffusion on current–voltage curves in potassium channels." *Discrete and Continuous Dynamical System Series B* **19**, 1837–1853 (2014).

[4] D. Andreucci, D. Bellaveglia, E.N.M. Cirillo, S. Marconi, "Monte Carlo study of gating and selection in Potassium channels." *Physical Review E* **84**, 021920 (2011).

[5] V.I. Arnold, "Ordinary Differential Equations." Third edition, Springer–Verlag, Berlin Heidelberg, 1992.

[6] J. Barrera, O. Bertoncini, R. Fernández, "Abrupt convergence and escape behavior for birth and death chains." *J. Stat. Phys.* **137**, 595–623 (2009).

[7] C. Bahadoran, T.S. Mountford, "Convergence and local equilibrium for the one–dimensional nonzero mean exclusion process." *Probability Theory and Related Fields* **136**, 341–362 (2006).

[8] L. Bertini, A. De Sole, D. Gabrielli, G. Jona–Lasinio, C. Landim, "Large deviations for the boundary driven simple exclusion process." *Math. Phys. Anal. Geom.* **6**, 231–267 (2003).

[9] R.A. Blythe, M.R. Evans, "Nonequilibrium steady states of matrix product form: a solver's guide." *Journal of Physics A: Math. Theor.* **40**, R333–R441 (2007).

[10] O. Chepizhko, E. G Altmann, F. Peruani, "Optimal noise maximizes collective motion in heterogeneous media." Phys. Rev. Lett. **110**(23):238101 (2013).

[11] E.N.M. Cirillo, A. Muntean, "Can cooperation slow down emergency evacuations?" *Comptes Rendus Macanique* **340**, 6260-628 (2012).

[12] E.N.M. Cirillo, A. Muntean, "Dynamics of pedestrians in regions with no visibility – a lattice model without exclusion." *Physica A* **392**, 3578–3588 (2013).

[13] A. De Masi, E. Presutti, E. Scacciatelli, "The weakly asymmetric simple exclusion process." *Annales de l'I.H.P., section B* **25**, 1–38 (1989).

[14] B. Derrida, M.R. Evans, V. Hakim, V. Pasquier, "Exact solution of a $1D$ asymmetric exclusion model using a matrix formulation." *Journal of Physics A: Mathematics and General* **26**, 1493–1517 (1993).

[15] N.G. van Kampen, "Stochastic Processes in Physics and Chemistry." Elsevier Science, 1981.

[16] B. Derrida, S.A. Janowsky, J.L. Lebowitz, E.R. Speer, "Exact solution of the totally asymmetric simple exclusion process: shock profiles." *J. Stat. Phys.* **73**, 813–842 (1993).

[17] A. De Masi, P. Ferrari, "Flux fluctuations in the one dimensional nearest neighbors symmetric simple exclusion process." *J. Stat. Phys.* **107**, 677–683 (2002).

[18] D. Desirable, P. Dupont, M. Hellou, S. Kamali–Bernard, "Cellular automata in complex matter." *Complex Systems* **20**, 67–91 (2011).

[19] P.A. Fedders, "Two–point correlation functions for a distinguishable particle hopping on a uniform one-dimensional chain." *Physical Review B* **17**, 40 (1978).

[20] F.J.M.M. de Gauw, J. van Grondelle, R.A. van Santen, "Effects of single–file diffusion on the kinetics of hydroisomerization catalyzed by Pt/H–Mordenite." *Journal of Catalysis* **204**, 53–63 (2001).

[21] M. Gorissen, A. Lazarescu, K. Mallick, C. Vanderzande, "Exact current statistics of the asymmetric simple exclusion process with open boundaries." *Phys. Rev. Lett.* **109**, 170601 (2012).

[22] K. Hahn, J. Kärger, "Deviations from the normal time regime of single–file diffusion." *Journal of chemical physics B* **102**, 5766–5771 (1998).

[23] K. Kosmidis, P. Argyrakis, P. Macheras, "A reappraisal of drug release laws using Monte Carlo simulations: the prevalence of the Weibull function." *Pharmaceutic Research* **20**, (7), 988–995 (2003).

[24] J. Krug, "Boundary–induced phase transition in driven diffusive systems." *Physical Review Letters* **67**, 1882–1885 (1991).

[25] A. Muntean, E.N.M. Cirillo, O. Krehel, M. Bohm, "Pedestrians moving in dark: Balancing measures and playing games on lattice." In "Collective Dynamics from Bacteria to Crowds", An Excursion Through Modeling, Analysis and Simulation Series: CISM International Centre for Mechanical Sciences, Vol. 553 Muntean, Adrian, Toschi, Federico (Eds.) 2014, VII, 177 p. 29 illus, Springer, 2014.

[26] F. Rezakhanlou, "Hydrodynamic limit for attractive particle systems on $\mathbb{Z}^d$." *Comm. Math. Phys.* **140**, 417–448 (1991).

[27] M.J. Simpson, K.A. Landman, B.D. Hughes, "Multi–species simple exclusion processs." *Physica A* **388**, 399–406 (2009).

[28] M.R. Evans, N. Rajewsky, E.R. Speer, "Exact solution of a cellular automaton for traffic." *Journal of Statistical Physics* **95**, 45–96 (1999).

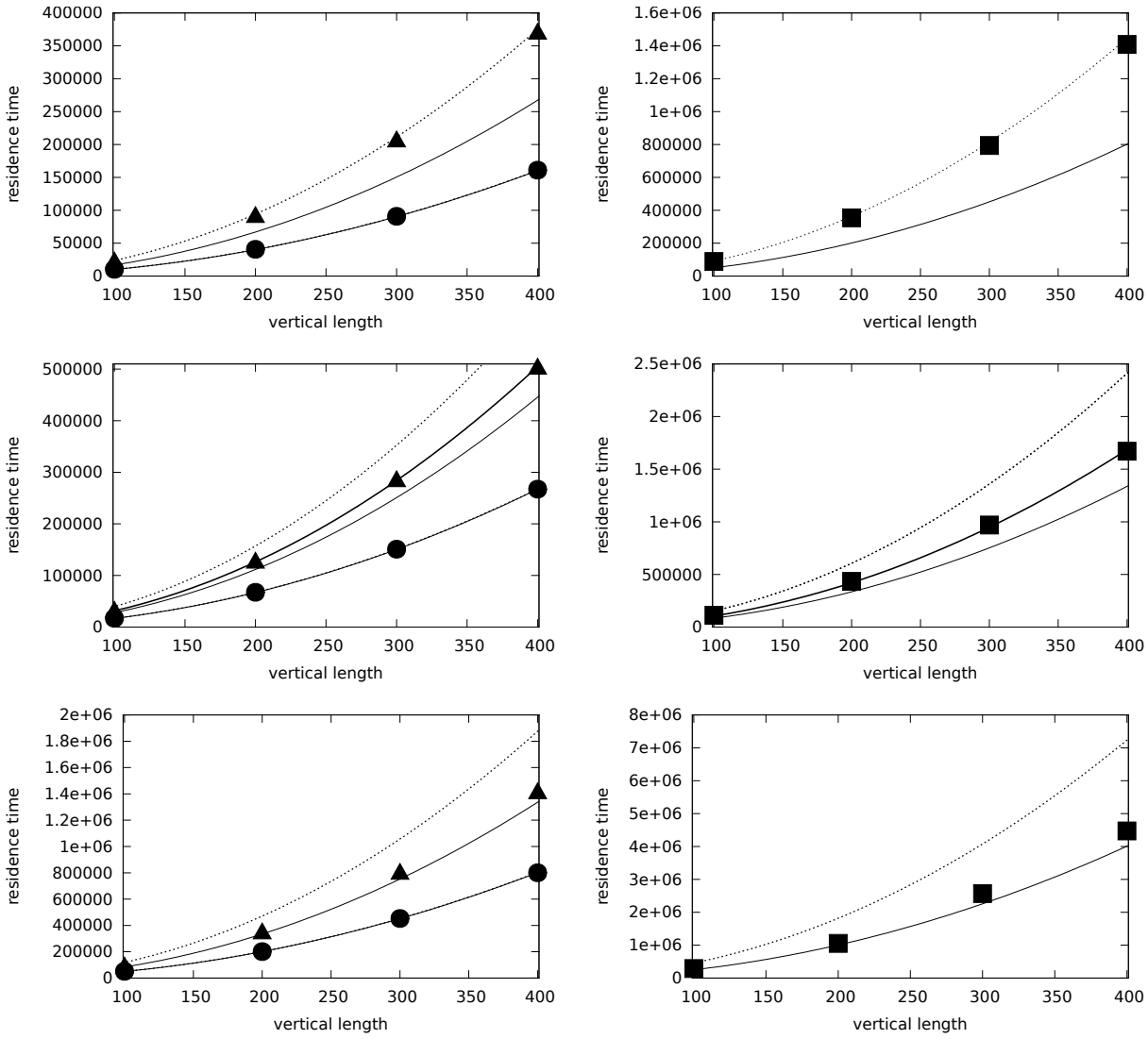

Figure 6.13: Residence time versus the vertical length of the strip L_2 in the case $\delta = 0$ and $h = 0, 0.4, 0.8$ from the top to the bottom. The symbols •, ▲, and ■ refer, respectively, to the cases $\varrho_{\rm d} = 0, 0.4, 0.8$. Solid thin lines are the theoretical prediction (5.32). Dotted lines are the Mean Field prediction (5.39). The solid thick lines are quadratic fitting of the experimental data: $3.16 \times L_2^2$ in the case $h = 0.4$ and $\varrho_{\rm d} = 0.4$ and $10.53 \times L_2^2$ in the case $h = 0.4$ and $\varrho_{\rm d} = 0.8$, The dotted and the solid lines corresponding to the cases $\varrho_{\rm d} = 0$ cannot be distinguished in the picture.

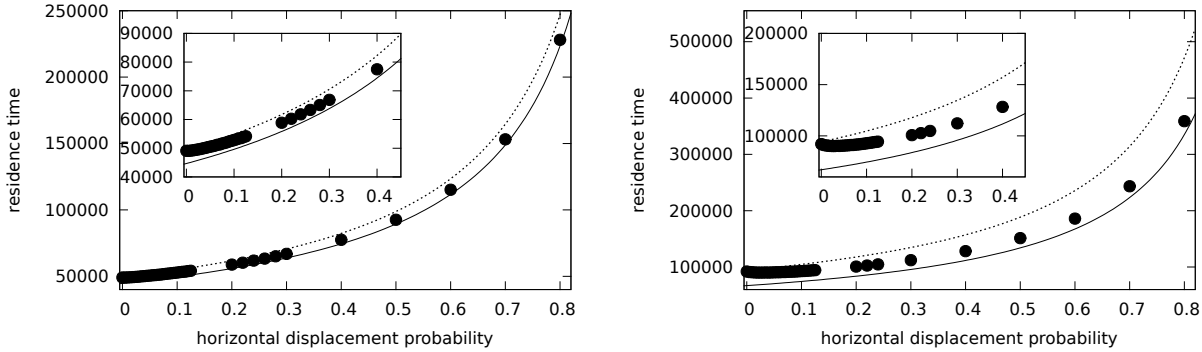

Figure 6.14: Residence time versus the horizontal displacement probability in the case $L_2 = 200$, $\delta = 0$, and and $\varrho_{\rm d} = 0.1$ (left) and $\varrho_{\rm d} = 0.4$ (right). Solid thin lines are the theoretical prediction (5.32). Dotted lines are the Mean Field prediction (5.39).

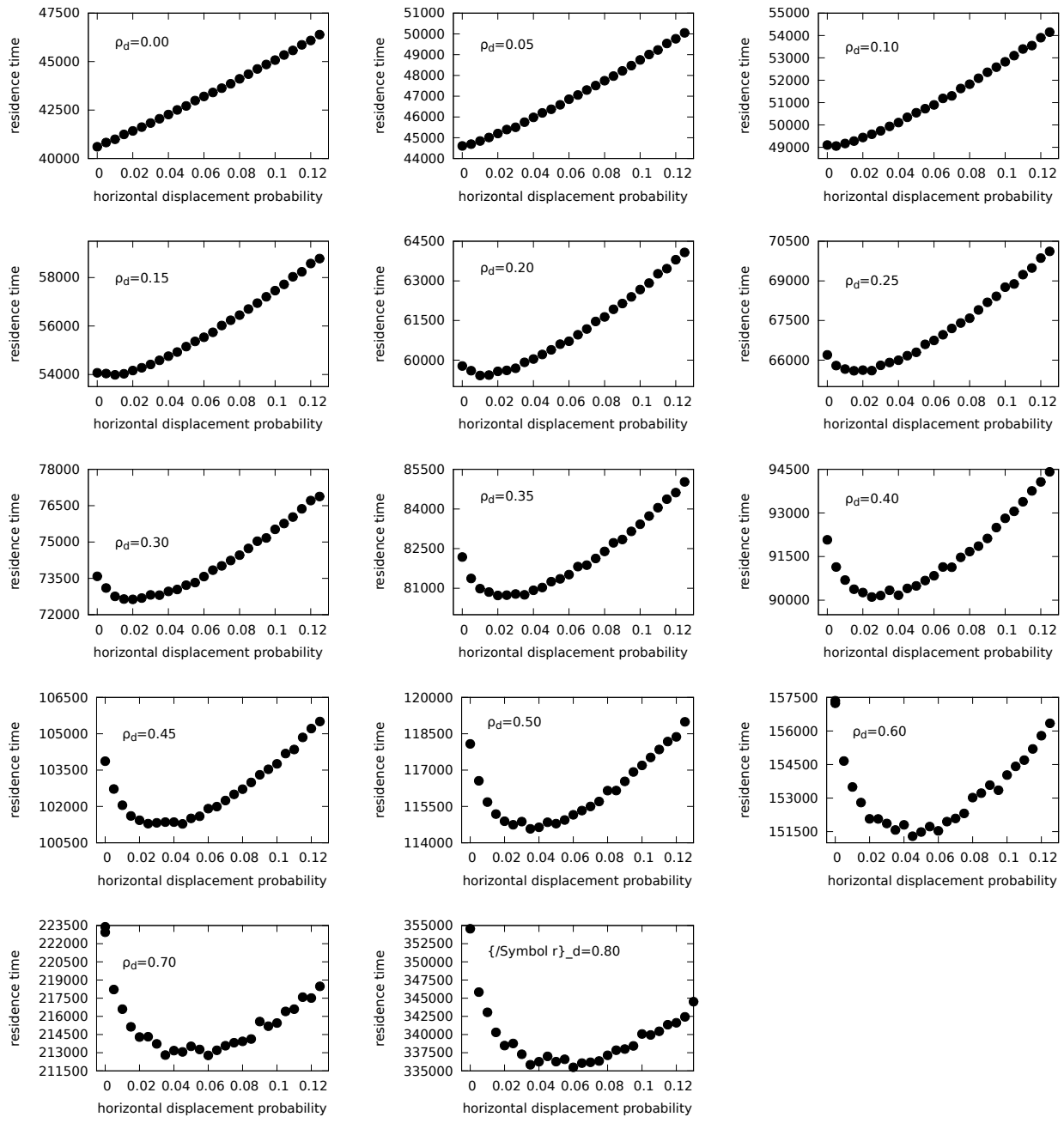

Figure 6.15: Residence time versus the horizontal displacement probability h in the case $\delta = 0$ and $L_2 = 200$. From the left to the right and from the top to the bottom the cases $\varrho_{\rm d} = 0, 0.05, 0.01, \ldots, 0.045, 0.5, 0.6, 0.7, 0.8$ are depicted.

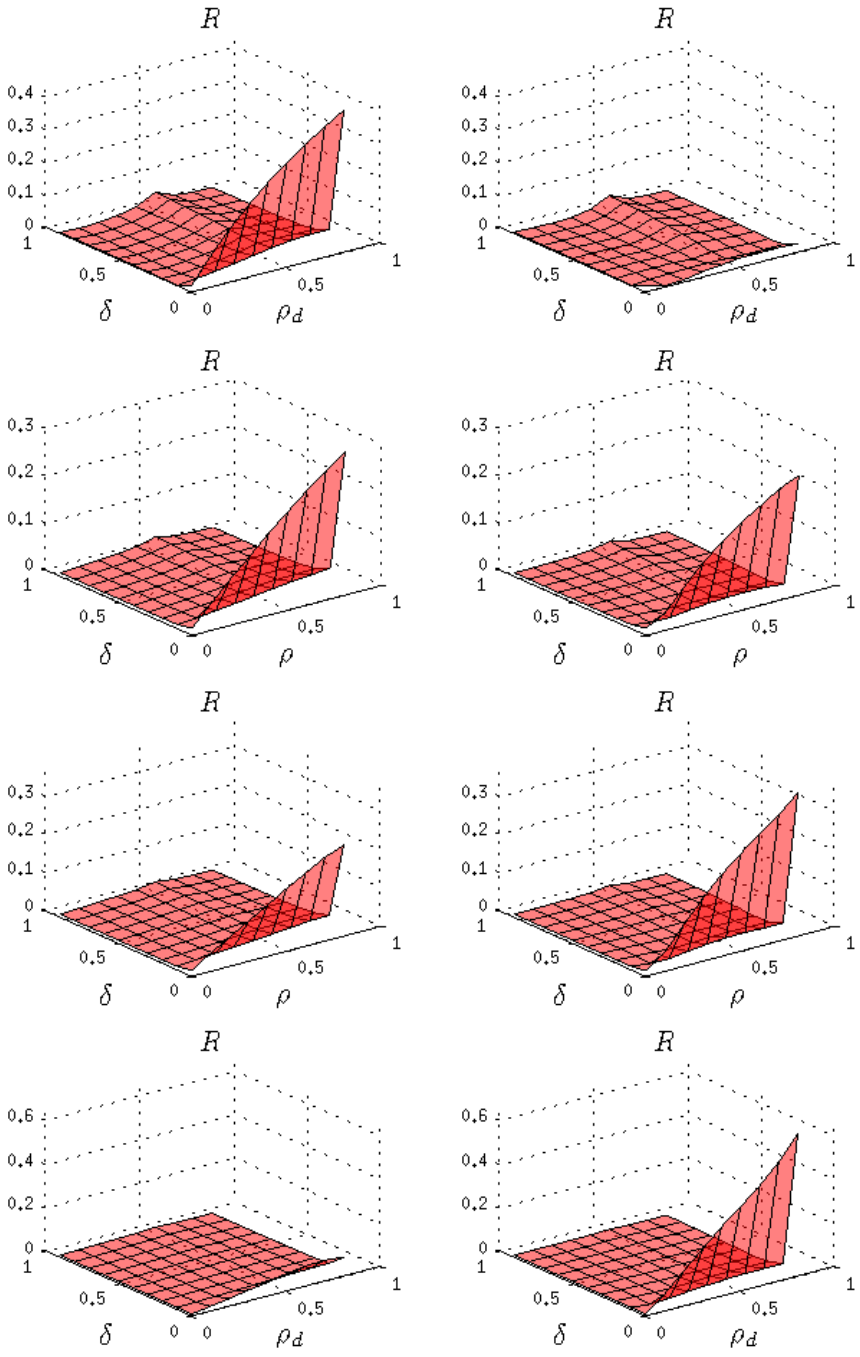

Figure 7.16: The difference (normalized with respect to the Monte Carlo measure) between the theoretical predictions (birth and death on the left and mean field on the right) and the Monte Carlo residence time measure is plotted as a function of δ and $\varrho_{\rm d}$ in the case $L_2 = 100$ and $\delta = 0$ for $h = 0, 0.2, 0.4, 0.8$ (from the top to the bottom).